Accepted Manuscript

Application of Reflectance Parameters in the Estimation of the Structural Order of Coals and Carbonaceous Materials. Precision and bias of measurements derived from the ICCP Structural Working Group

S. Pusz, A. Gomez-Borrego, D. Alvarez, I. Camean, V. du Cann, S. Duber, W. Kalkreuth, J. Komorek, J. Kus, B. Kwiecińska, M. Libera, M. Marques, M. Misz-Kennan, R. Morga, S. Rodrigues, Ł. Smedowski, I. Suarez-Ruiz, J. Strzezik

PII: S0166-5162(14)00074-3
DOI: doi: 10.1016/j.coal.2014.04.004
Reference: COGEL 2286

To appear in: *International Journal of Coal Geology*

Received date: 18 February 2014
Revised date: 8 April 2014
Accepted date: 9 April 2014

Application of Reflectance Parameters in the Estimation of the Structural Order of Coals and Carbonaceous Materials. Precision and bias of measurements derived from the ICCP Structural Working Group.

S. Pusz[1]*, A. Gomez-Borrego[2], D. Alvarez[2], I. Camean[2], V. du Cann[3], S. Duber[4], W. Kalkreuth[5], J. Komorek[6], J. Kus[7], B. Kwiecińska[8], M. Libera[1], M. Marques[9], M. Misz-Kennan[4], R. Morga[6], S. Rodrigues[9, 10], Ł. Smędowski[11], I. Suarez-Ruiz[2], J. Strzezik[12]

[1] *Centre of Polymer and Carbon Materials, PAS, M. Curie-Skłodowskiej 34, PL-41819 Zabrze, Poland, spusz@cmpw-pan.edu.pl*
[2] *Instituto Nacional del Carbón, CSIC, PO Box 73, 33080 Oviedo, Spain*
[3] *Petrographics SA, Suite 155, Private Bag X 025, Lynnwood Ridge, Pretoria 0040, South Africa*
[4] *University of Silesia, Faculty of Earth Sciences, Bedzinska 60, PL-41200 Sosnowiec, Poland*
[5] *Instituto de Geociências, UFRGS, Av. Bento Gonçalves, 9500, 91501-970 Porto Alegre, RS, Brazil*
[6] *Institute of Applied Geology, Silesian University of Technology, Akademicka 2, PL-44100 Gliwice, Poland*
[7] *Bundesanstalt für Geowissenschaften und Rohstoffe GEOZENTRUM, Stilleweg 2, D-30655 Hannover, Germany*
[8] *AGH-University of Science and Technology, Al. Mickiewicza 30, PL-30059 Krakow, Poland*
[9] *Faculdade de Ciências da Universidade do Porto Rua do Campo Alegre, 687, 4169-007 Porto, Portugal*
[10] *School of Earth Sciences, University of Queensland, Steele Building, St Lucia, 4072 QLD, Australia*
[11] *Institute for Chemical Processing of Coal, 1 Zamkowa St; PL-41803 Zabrze; Poland*
[12] *Department of Physical Chemistry and Technology of Polymers, Silesian University of Technology, Strzody 9, PL-44100 Gliwice, Poland*

Abstract

Optical reflectance of vitrinite is one of the fundamental physical properties that have been used for the study of coal and carbonaceous materials. Organic matter in coals and carbonaceous matter consists mainly of aromatic lamellae, whose dimensions and spatial orientation define its internal structure. Various reflectance parameters describe well the average degree of order of the molecular structure of organic matter. Moreover, reflectance parameters are numerical values which characterize the samples unambiguously, facilitating the comparison of the optical properties of different carbonaceous materials as well as comparison between optical parameters and other physical or chemical factors.

The focus of this study is the evaluation of the precision and bias of reflectance measurements (R_{max} and R_{min}) performed by various analysts in different laboratories in order to check the applicability of reflectance parameters to the estimation of the structural order of coals and carbonaceous materials. Additionally, it was desirable to compare reflectance parameters with other parameters obtained by different analytical methods able to provide structural information. The consistency and repeatability of the reflectance measurements obtained by different participants turned out to be such as to enable the drawing of similar conclusions regarding the structural transformation of anthracite during heating.

Corresponding author (S. Pusz): Tel. +48 32 271 60 77; fax: +48 32 271 29 69.
E-mail address: spusz@cmpw-pan.edu.pl

Good correlations were found between the reflectance parameters studied and structural factors obtained by comparative methods. The reflectance parameters examined proved to be very sensitive to any changes of the structural order of coals and carbonaceous materials and seem to be a perfect complement to structural studies made by X-ray diffraction or Raman spectroscopy.

Key Words: *reflectance parameters; structural order; anthracite;XRD, Raman spectroscopy, TEM*

1. Introduction

Optical reflectance of macerals is one of the fundamental physical properties that have been used in the study of coal and carbonaceous materials. In practice, coal reflectance is understood as the reflectance of vitrinite – the maceral dominant in most coals and principally responsible for the behavior of coals in technological processes such as carbonization, coking, gasification and liquefaction. Vitrinite reflectance increases progressively with increasing degree of coalification and is regarded as perhaps the best single parameter of coal rank (Stach et al., 1982; ISO 11760:2005). Different relationships between the reflectance and chemical-rank parameters including volatile matter, carbon content, hydrogen content, atomic ratio H/C have been found (Chruściel, 1981; Davis, 1978; Stach et al., 1982, McCartney and Teichmüller, 1972; van Krevelen, 1993).

Measurements of vitrinite reflectance in polarized light reveal an anisotropy that is related to the degree of ordering of the molecular structure of this maceral (Davis, 1978; Goodarzi and Murchison, 1978; Murchison, 1978). Later studies have shown that the optical features of vitrinite depend on the strength and directions of tectonic pressures occurring in a coal basin during maturation. If only lithostatic pressure occurs, vitrinite is considered to be uniaxial negative. If any oriented pressures (tectonic strains and shears) occur in the basin, optical properties of vitrinite can change to biaxial negative or even biaxial positive (Cook et al., 1972; Goodarzi, 1985; Langenberg and Kalkreuth, 1991; Levine and Davis, 1989; Ross and Bustin, 1997; Stone and Cook, 1979; Ting, 1981;). Vitrinite reflectance is used in a number of applications such as determination of the degree of coal metamorphism (Hower and Davis, 1981a, 1981b; ISO 11760:2005), the evaluation of technological properties (Suarez-Ruiz and Crelling, 2008), and in basin analysis to define the maturity level of the organic matter in relation to oil and gas occurrences (Bertrand and Malo, 2012 and references therein; Kalkreuth and McMechan, 1996; Laxminarayana and Crosdale, 1999; Li et al., 2006).

The organic matter of coals and carbonaceous materials consists mostly of aromatic lamellae with non-aromatic functional groups and heteroatoms with pores interspersed among them (van Krevelen, 1993). With increasing coal rank, single aromatic layers form stacks of 2-3 aromatic lamellae almost parallel one to another. These stacks, together with the surrounding non-aromatic components are called Basic Structural Units (BSU) (Blanche et al., 1995). The dimensions and spatial orientation of BSUs define the internal structure of coals and carbon materials. If there is no clear direction of spatial orientation, the structure is isotropic. However, in most carbon materials and coals of higher rank (Alpern and Lemos de Souza, 1970) a preferential orientation of the BSUs exists forming anisotropic patterns.

The structural order of coals and carbonaceous materials can be well illustrated by a three-dimensional ellipsoid termed the Reflectance Indicating Surface (RIS). The principal RIS axes, *i.e.*, R_{MAX}, R_{INT} and R_{MIN} (Fig. 1) correspond to the axes of the symmetry and define the optical character of materials studied as uniaxial negative when $R_{MAX}=R_{INT} > R_{MIN}$, uniaxial positive when $R_{MAX} > R_{INT} = R_{MIN}$, biaxial negative when $R_{MAX} > R_{INT} >> R_{MIN}$, biaxial positive when $R_{MAX} >> R_{INT} > R_{MIN}$ and biaxial even when $R_{INT} = R_{MAX} + R_{MIN}/2$ (Hevia and Virgos, 1977; Ting, 1981).

Initially, RIS axes were determined from measurements of maximum- and minimum reflectance values on three mutually perpendicular surfaces of coal blocks. This method was troublesome and, in practice, was used only to determine the direction of lithostatic pressure or tectonic strains and shears in coal deposits (Hower and Davis, 1981a; Levine and Davis, 1989; Langenberg and Kalkreuth, 1991). Kilby (1988, 1991) proposed a method for determining the optical character of coal on the basis of measurements of apparent maximum (R'_{max}) and apparent minimum (R'_{min}) reflectance values of non-oriented coal grains. This method made possible the reconstruction of the RIS of powdered samples (Duber et al., 2000; Grieve, 1991). The three principal axes of a RIS are then determined by means of a graphical method which involves plotting measured R'_{max} and R'_{min} values versus bireflectance (R'_{bi}), where $R'_{bi} = R'_{max} - R'_{min}$, at a given point of measurement (Fig. 2). Reflectance parameters obtained from the results of the measurements, i.e., mean maximum reflectance (R_{max}),mean minimum reflectance (R_{min}) and mean bireflectance (R_{bi}), define the average degree of order of the molecular structure of the organic matter. R_{max} corresponds to the dimensions of carbon layers, whereas R_{min} expresses the degree of order of carbon layers along the Z-axis (carbon stacks). R_{bi}, a parameter depending on R_{max} as well as R_{min} values, represents the dimensions and spatial arrangement of the basic structural units of coals or carbonaceous materials (Murchison, 1978). Based on RIS axes R_{MAX}, R_{INT} and R_{MIN}, more complex reflectance parameters, *i.e.*, Kilby RIS parameters R_{ev}, R_{st} and R_{am} (Kilby, 1988, 1991) can be calculated

to describe the internal structure of coal or carbonaceous materials in more detail. The parameter R_{ev} (RIS equivalent volume) is the radius value of a spherical RIS with a volume equal to the given RIS. The parameter R_{st} determines the optical character (RIS style) with a value that ranges from -30 to +30. When the R_{st} is +30 or -30, the character of the RIS is uniaxial positive (+) or negative (-) respectively. Values between -30 and +30 indicate either a biaxial negative or positive character. The parameter R_{am} characterizes RIS anisotropy and informs about the elongation of the RIS shape. $R_{am} = 0$ when $R_{MAX} = R_{INT} = R_{MIN}$ (sphere) and the character of the structure of the material being studied is isotropic.

The reflectance parameters mentioned above have been successfully used to follow the transformations of anthracites under slow heating rate carbonization conditions (Pusz et al., 2002, 2003; Suárez-Ruiz and Garcia, 2007; Rodrigues et al., 2011) and under high heating rate combustion conditions (Borrego and Martin, 2010), providing a very good numerical measure of the optical characteristics of the material that could also be applied to the estimation of the degree of their structural order. In contrast, while the measurement of random and maximum reflectances of vitrinite are described by standards (ISO 7404-5:2009 and ASTM D2798 - 11), which establish the repeatability and reproducibility limits, the scattering of bireflectance measurements have not been so far assessed. A measurement of the precision of R'_{max} and R'_{min} measurements by various analysts in different laboratories is required to confirm the applicability of these parameters.

At the 53rd ICCP Meeting in Copenhagen (Denmark, 2001), the *Working Group on Application of Reflectance for Estimation of Structural Order* (Structural WG) was established. In the years 2001-2011, this working group performed a 3-stage round-robin exercise consisting of the study of changes in the reflectance parameters of high rank meta-anthracite during thermal treatment at a variety of temperatures ranging from ambient temperature up to 2000°C.

The approach used was based on the work by Duber et al. (2000) and Pusz et al. (2002, 2003). The round-robin exercise involved 18 participants from 6 countries, thirteen of whom measured reflectance values – seven participants for each stage of the exercise, except for experiments at the temperature 450ºC and 700ºC, where five analysts participated (Table 1). Comparative analyses of reflectance parameters were conducted to estimate the precision of the measurements and the scatter of the calculated parameters, in order to determine the uncertainty associated with the use of reflectance parameters to evaluate the degree of structural ordering of coal and carbonaceous material.

The results of the optical investigations were related to those of structural studies made by X-ray Diffraction (XRD), Raman spectroscopy and transmission electron microscopy (TEM).

2. Experimental

2.1 Sample and sample preparation

High rank meta-anthracite Svierdlovski (SV) from DONBAS in Ukraine (Stach et al., 1982) composed of vitrinite – (94.9 vol. %), inertinite, (4.9 vol. %), liptinite (0 vol. %), mineral matter (0.2 vol. %), and with a mean maximum reflectance R_{max} = 6.90 %, was heated in an inert atmosphere with a heating rate of ~5-10^{o}C per minute to various temperatures ≤ 2000^{o}C. The final temperature was held for 1 hour before cooling the sample in an inert atmosphere to room temperature.

The round-robin exercise was conducted in three stages:

Stage I (2003) involved the analysis of the raw anthracite and samples heated at temperatures of 450^{o}C, 700^{o}C and 950^{o}C,

Stage II (2008-2011) involved anthracite samples heated at temperatures of 1400^{o}C, 1700^{o}C and 2000^{o}C,

Stage III (2009) involved anthracite samples heated at temperatures of 1500^{o}C, 1600^{o}C and 1650^{o}C.

Pellets provided to participants were prepared according to the procedure recommended by the ICCP (Stach et al., 1982). Special attention was given to the thorough mixing of the anthracite grains with the epoxy resin to assure a random distribution of grains. The pellets were ground with progressively finer grades of wet SiC papers from 200 to 1000 grit. For the polishing procedure, diamond products of 3µm, 1µm and ¼ µm sizes were used due to the hardness of the samples.

2.2 Procedures for vitrinite reflectance measurements and data treatment.

All participants were asked to measure R'_{max} and R'_{min} reflectance values of according to the conventional method described in ISO standard 7404-5:1994. A minimum of 200 measurement points per sample were carried out on vitrinite grains using monochromatic, polarized light of wavelength λ=546 nm, with immersion oil (refractive index = 1.518 at a temperature of 23^{o}C ± 2^{o}C). Reflectance standard SiC (Zeiss, mean random reflectance in immersion oil R^{oil} = 7.43%) was recommended for calibration of the microscopes for high reflectance measurements. R'_{max} and R'_{min} reflectance values were recorded at the same point during rotation of the microscopic stage or a sample through 360^{o}. Each measurement was

made on a separate vitrinite particle. **While** manual- and automated methods of reflectance measurement were allowed, all participants used a manual method.

Based on the results of the reflectance measurements delivered by participants, mean R_{max} and R_{min} values and principal RIS axes (R_{MAX}, R_{INT}, R_{MIN}) were determined. Afterwards, other reflectance indicators were calculated, *i.e.* R_{bi} and Kilby's parameters R_{ev}, R_{st} and R_{am}.

The statistics used for the assessment of the results were similar to those applied in the ICCP Accreditation Programs (ICCP, 2014). Signed multiple of the standard deviation(SMSD) is a measure of the sign and amount of bias expressed as the distance to the group mean:

$$SMSD = \frac{(x_i - \bar{x})}{\sigma}$$

where x_i is the individual's mean for a given parameter, $\bar{x}$ is the group mean and σ is the group standard deviation. The Unsigned multiple of the standard deviation (UMSD) is the absolute value of SMSD and is considered as a measure of the precision. The coefficient of variation (CV=100*σ/$\bar{x}$) allows comparison of the scattering of populations with different mean values. The average values for the UMSD (AUMSD) were also taken into account for the evaluation of the results.

According to Jenkins (2003), SMSD value < ±1.0 indicates consistent results, whereas SMSD >±1.0 indicates an improvement is needed in the method being used. In the case of UMSD, the value 1.5 is the threshold established as acceptable for reflectance measurement accreditation programs (~ 80% of normal distribution) (ICCP, 2014).

2.3 Methods of comparative structural studies

2.3.1 XRD

XRD technique provides information about the size of the crystallites which make up the ordered structure of coal and carbon materials. The XRD parameters usually quoted are: interlayer spacing (d_{002}), stack height (L_c) and stack width (L_a).

The XRD analyses were made in Instituto Nacional del Carbon, CSIC, Oviedo, Spain. The diffractograms were recorded using a Bruker D8 powder diffractometer equipped with a monochromatic Cu Kα X-ray source and an internal standard of silicon powder. Diffraction data were collected by a step-scanning method with scan step of 2 s, for 2θ = 10 – 90^o. The mean interlayer spacing, d_{002}, was evaluated from the position of the (002) peak by applying Bragg's equation. The mean crystallite sizes, L_c and L_a, were calculated from the (002) and (110) peaks respectively, using the Scherrer formula, with values of K = 0.9 for L_c and 1.84 for L_a. Any broadening of diffraction peaks due to instrumental factors was corrected with the

use of a silicon standard (Rodrigues et al., 2013). The XRD factors were determined with the standard errors: < 0.04 % for d_{002}, < 1.4 % for L_c and < 6.0 % for L_a.

2.3.2 Raman Spectroscopy

Raman spectra of coal and carbonaceous materials exhibit two evident bands from ordered- and disordered regions. The first band at 1580 cm^{-1} (*G1* band) attributed to the stretching vibration mode with E_2g symmetry of polyaromatic structures C-C of graphite and the second at 1350 cm^{-1} (*D1* band) associated with disordered, sp^3-hybridized carbon attributed to in-plane defects in the graphene sheets or the occurrence of heteroatoms (Morga, 2011). The ratio of *D1*band/*G1*band is the most common Raman parameter illustrating the structural order of coal and carbonaceous materials. The lower the value of *D1/G1*, the better ordered the structure of the material studied (Beyssac et al., 2003; Guedes et al., 2010). Additionally, in Raman spectra of highly metamorphosed coals and carbon materials, there are 2*D* bands at about 2600 cm^{-1} that are overtones of the *D1* band. According to Potgieter-Vermaak et al. (2011), the 2*D* band corresponds to the lack of in-plane defects in carbon planes making them stiff and perfect.

The Raman spectra were recorded at the Silesian Technical University (Gliwice, Poland) on a Renishaw inVia spectrometer coupled with a Leica DM 2500M microscope. The HeNe laser beam operating with an excitation λ = 633 nm and the maximum laser power was 17 mW. The measurement parameters were as follows: laser power – 0.17 mW (1% of maximum power), time of exposure – 10 s, number of scans – 7, acquisition range – 100-3200 cm^{-1}. For each sample, 7-10 points were analyzed to obtain an insight into the structural heterogeneity of the sample.

2.3.3 TEM

TEM has been used to study the multiscale organization of anthracites since the 1980s. It was found that anthracites comprise of polyaromatic BSUs, nanometric in size, which have a tendency to join and form molecular oriented domains (Oberlin 1984). With increasing metamorphism or during experimental treatment with high temperature and pressure, the dimensions of the domains increase and their arrangement develops along a preferential plane; this is responsible for the total anisotropy of anthracites (Rouzaud and Oberlin 1990). These effects can be observed on TEM images. In a dark field TEM mode (DF), the BSUs are visible as bright dots, and the domains as aggregates of dots. Bigger aggregates indicate greater domains characteristic of a better-ordered structure. The structural order of anthracite can be also illustrated by the diffraction pattern of scattered electrons. High resolution

transmission electron microscopy (HRTEM) can provide direct images of the arrangement of carbon planes in the anthracite structure.

The TEM studies were conducted at the University of Silesia (Sosnowiec, Poland) using a PHILIPS EM400T with a magnification of 23,000× and an acceleration voltage of 100 kV, by using bright field (BF) and the 002DF techniques of observation.

The HRTEM investigations were carried out in the Centre of Polymer and Carbon Materials Polish Academy of Sciences (Zabrze, Poland), using a Tecnai F20 microscope (FEI Company) equipped with field emission gun, operating at an acceleration voltage of 200 kV. Images were recorded on the Eagle 4k HS camera (FEI Company) and processed with TIA software (FEI Company).

The samples for the TEM studies were ground in ethanol in a mortar. The suspension was then placed on a cooper grid 300 mesh (Quantifoil, Germany)and the alcohol evaporated before the specimens were placed in the microscope column and analyzed.

3. Results and discussion

3.1 Reflectance measurements

Table 2 presents the R_{max} and R_{min} reflectances of raw anthracite and respective heat treated materials studied. The average R_{max} values increase regularly from 6.90% in the raw sample up to 11.85% in the sample heated to 2000 ºC, whereas the average R_{min} values change from 4.51% in the raw sample to 2.86% in the sample heated to 2000 ºC. Figure 3 shows the mean R_{max} and R_{min} values of the samples studied and the average standard deviation of measurements of apparent R'_{max} and R'_{min} made by every participant. It is evident that the average R_{max} and associated standard deviation increase gradually with rising temperature. The mean standard deviation is quite low at temperatures < 950ºC, somewhat higher in the range 1400-1650ºC and distinctly higher at temperatures > 1700ºC. The mean R_{min} also increases with rising temperature up to 1400ºC, then drops slightly between 1500-1650ºC before falling rapidly above 1700ºC, whereas the standard deviation of R'_{min} measurements increases progressively over the entire range of temperatures. In addition to the increase in standard deviation, which is always associated to the increase of the values of the mean, the changes in the standard deviations of R'_{max} and R'_{min} reflect the transformation in the structure of the anthracite, which leads to increasing range of values of individual reflectance parameters

(Fig.3). The standard deviations of individual sets of data are significantly higher for R_{min} than for R_{max}.

The CV allows the comparison of the scatter of values for populations with different means and therefore CV values for R_{max} and R_{min} were calculated. The CVs of R_{max} are considerably lower than those of R_{min} and vary only slightly through the whole temperature interval. The marked rearrangement in structural order which results in only a slight elevation of R_{max} but drastically lowers the R_{min} value between 1650-1700°C (Fig. 3), hardly affects the CVs of R_{max}, whereas those of R_{min} increase abruptly from 43.64 at 1650°C to 118.0 at 1700°C. Any changes in CVs below 1650°C and above 1700°C are almost negligible (Fig. 4). A sudden increase in CVs for R_{min} suggests drastic transformations in the structure of anthracite over 1650 °C, whose structure is difficult to stabilize in the short holding time of these experiments, resulting in a large scatter of measurements.

The assessment of the dispersion of R'_{max} and R'_{min} measurements around the mean is better performed through the analysis of SMSD and UMSD results. Most of the UMSD values obtained in the exercise (Fig. 5) are comfortably below 1.5 – the acceptable limit for reflectance measurements according to the ICCP Accreditation Programs. The number of UMSDs > 1.5 is 14.4% of the total. However, only 6 cases (4.55%) seem to be random errors. That is, when among all UMSD values calculated for an individual participant, only one is > 1.5 and the final mean UMSD, *i.e.* AUMSD, is < 1. The others cases (9.85%) belong to participants 5, 7, 8 and 12; almost all their UMSD values are distinctly > 1.5 or ~ 1.5. Their AUMSDs are > 1, some even > 1.5 (Table 3). This situation is indicative of a systematic error due to, *e.g.*, microscope setup or calibration, the reflectance standard used, specimen preparation, etc. This can be confirmed by the instance where the results of measurements became worse after changing microscope equipment during the course of the exercise.

Most of the SMSD values are consistent with reliable measurements (73.5% SMSD < ±1.0), 12.1% required little correction (± 1.0 < SMSD < ±1.5) and only 14.4% indicated problems with measurement technique (SMSD ≥ 1.5) (Table 3). In general, the results of the measurements of R'_{max} and R'_{min} of various analysts from different laboratories scatter reasonably and support similar conclusions. Serious deviations observed for 4 participants (participant 12/I Stage, 8/II Stage, 5, 7/III Stage) constitute < 10% of all the results. Besides, they seem to be systematic errors caused by equipment set up or measurement technique and can be eliminated more readily than can random errors.

3.2 Reflectance parameters calculated from R'_{max} and R'_{min} measurements

Calculated reflectance parameters derived from the R'_{max} *and* R'_{min} values are shown in Table 4. The values of R_{MAX} and R_{INT} are close to each other and considerably higher than R_{MIN} indicating a RIS that is clearly biaxial negative (Table 4, Fig 6). This structure is

maintained almost to 1700 ºC, where increasing differences between the three axes are observed. The R_{MAX} value, and the anisotropy parameters R_{am} and R_{bi}, increase progressively in the interval 700- 1650 ºC and then rapidly at 1700ºC. R_{MIN} and R_{ev} values increase gradually from 700 to 1650ºC and then decrease abruptly at 1700ºC. R_{INT} that is depended on R'_{max} and R'_{min} measured values, increases gradually between 700 and 1400 ºC and then maintain similar values up to 2000 ºC, because the increase of R'_{max} is balanced with the strong decrease of R'_{min} (Table 4).

The R_{st} parameter scarcely changes till the temperature 1650 ºC (Table 4, Fig. 7a). Its values, contained in the range from -12.0 to > -18.0, indicate a biaxial negative optical character of the samples (Fig.7b). Higher values of R_{st} were determined only for participants 5 and 12, whose results of measurements of R'_{max} and R'_{min} have the greatest bias to the group mean. At the temperature of 1700ºC the optical character of samples studied changes distinctly that make impossible the calculation of average values of the R_{st} parameter for samples SV1700 and SV2000. The crossplots of these samples, determined from the results of measurements, show coexisting uniaxial positive and biaxial components in the single sample (Fig. 7c). Prior research suggested that a change in R_{st} parameter is caused mainly by high environmental pressure - geological or experimental (Grieve, 1991; Ross and Bustin, 1997, Wilks et al., 1993), whereas temperature has secondary influence (Pusz et al., 2002; Suarez-Ruiz and Garcia, 2007). These results show that sufficiently high temperature with ambient pressure only can also transform the structure of organic matter in such a way that its optical character changes significantly.

The dispersion of parameters calculated on the basis of reflectance measurements, *i.e.*, RIS axes: R_{MAX}, R_{INT} and R_{MIN}, Kilby's parameters R_{ev}, R_{st}, R_{am} and R_{bi}, is primarily a consequence of the scatter in the measured R'_{max} and R'_{min} values (Table 2 and 4). Nevertheless the calculation procedures could have an incremental or detrimental effect on the parameters**.** This was checked by comparing the data in Tables 3, 5 and 6, where it is observed that generally speaking, values within similar intervals for AUMSD are obtained for the raw measurements (R_{max} and R_{min}) and the calculated parameters (R_{MAX}, $R_{INT,}$ $R_{MIN,}$ $R_{ev,}$ R_{st}, $R_{am,}$ R_{bi}). This is not the case for the analysts that showed differences in their performance, and some of them (participant 5 and 12) show systematically high values for AUMSD. No clear relationship could be found for any parameter or measurement to have systematically higher or lower AUMSD values but the dispersion in the parmeters (Tables 5 and 6) is clearly higher for those participants whose scattering of R'_{max} and R'_{min} measurements is greater (Table 2). Figure 8 shows the UMSD values of RIS axes determined from the measurement data of the participants. UMSDs ≥1.5 amount to 12.5 % of the total and are distributed equally

for each axis. The data from two participants (5 and 12) support an AUMSD > 1.5. The UMSD values of other reflectance parameters (R_{ev}, R_{st}, R_{am} and R_{bi}) are presented on Fig. 9. Some 11.4 % of these are > 1.5. In this case, the AUMSD values > 1.5 derive from the same participants (5 and 12). SMSD values indicating reliable results amount to > 70% with regard to RIS axes (Table 5) and > 85 % with regard to R_{ev}, R_{st}, R_{am} and R_{bi} (Table 6). These results are similar to those obtained for the measurement data.

3.3 Reflectance parameters of Svierdlovski anthracite in relation to structural factors obtained with comparative methods

3.3.1 X-ray Diffraction

The XRD parameters of the anthracite studied changed subtly up to a temperature 1400^{o}C. Above that, in the range 1500-1650^{o}C they increased only marginally (L_a and L_c) or decreased (d_{002}) before changing rapidly at 1700^{o}C.

The mean R_{max} and maximum RIS axis (R_{MAX}) correspond well to the L_a parameter representing the dimensions of the carbon lamellae. The trends in changes of all these parameters are similar (Fig.10). However, up to a temperature 1650^{o}C, R_{max} and R_{MAX} values increase much more strongly than those of L_a parameter. This is the effect, on one hand, of the lateral development of graphene layers, well illustrated by the L_a parameter and, on the other, of the arrangement of small organic layers along the preferential direction, reflected by R_{max} and R_{MAX} but not by L_a.

The mean R_{min} and R_{MIN} values show a similar trend with increasing temperature as the d_{002} parameter obtained with X-ray diffraction (Fig. 11). However, where d_{002} values decrease significantly in the temperature range 1400-1650^{o}C, reflectance parameters decrease only slightly. This discordance appears, because the d_{002} parameter reflects interlayer spacing in graphene stacks, whereas R_{min} and R_{MIN} express interlayer spacing in stacks as well as the spatial orientation of stacks due to preferential direction. Eventually, R_{min} and R_{MIN} decrease significantly only when interlayer spacing in stacks become small enough and the carbon planes are arranged sufficiently parallel.

Anisotropy parameters R_{bi} and R_{am} show similar trends with increasing temperature as the L_a and L_c values representing the dimensions of organic layers and the height of stacks of these layers (Fig. 12) and they are also inversely proportional to the interlayer spacing expressed by the d_{002} factor (Fig 13).

Reflectance parameters give quite similar, but not identical information about the structure of materials studied as do the XRD factors. The former are even more sensitive to any changes in the sizes and spatial orientation of carbon layers.

3.3.2 Raman Spectroscopy

The Raman spectra of the Svierdlovski anthracite change significantly with temperature of treatment (Fig. 14). They confirm the transformations of the anthracite structure previously determined by reflectance studies. The ratios *D1/G1* increase progressively up to 1650^{o}C and then decreases rapidly at 1700^{o}C and 2000^{o}C, reflecting the abrupt transformation of the anthracite structure from turbostratic to graphite-like. In addition, for samples heated to 1700^{o}C and 2000^{o}C, sharp *2D* bands characteristic of well-ordered carbon structures appear. The changes of integrated areas ratio of *D1* (A_{D1}) and *G1*(A_{G1}) bands correlate very well with the changes of R_{min} values (Fig. 15a). Furthermore, the A_{D1} and A_{G1} values decrease with increasing temperature of treatment of the anthracite as R_{max} values increase (Fig. 15b).

3.3.3 Transmission Electron Microscopy

Gradual increase in the degree of structural order in Svierdlovski anthracite during heating to 2000 ºC, visible in the TEM micrographs, confirm the trend of the reflectance parameters changes. Increasing degree of order of carbon layers of the anthracite as a result of experimental temperature increase is also confirmed by diffraction patterns of electrons illustrating mutual arrangement of carbon atoms (Fig. 16).

The progressive growth of bright areas in the dark field TEM images is related to the domain dimension increase and also correlates to reflectance parameters changes.

4. Conclusions

- The precision of measurements of R'_{max} and R'_{min} of the raw and thermally treated anthracite samples made by contributing participants seems to be reasonable. The UMSD values are mostly < 1.5 and AUMSD values < 1.0. The corresponding SMSD valuesindicate a good degree of consistency in the results.
- The increase observed in the standard deviation of R'_{max} and R'_{min} measurements due to experimental temperature increasing is not only attributable to the increase in absolute reflectance values but also to the increase in the range of values of reflectance parameters, as illustrated by their coefficients of variation.
- Calculated reflectance parameters, *i.e.,* RIS axes, Kilby's parameters R_{ev}, R_{st} and R_{am} and bireflectance R_{bi} also scatter reasonably, showing a similar degree of scattering as

the measured values. The UMSDs of individual participants are mostly < 1.5. The AUMSD values are all < 1.5 and most < 1.0.

- The accuracy and reproducibility of reflectance measurements made by different participants in different laboratories allows similar conclusions to be drawn regarding the structural transformation of coals or carbonaceous materials.
- Good relationships were found between the reflectance parameters studied and structural factors obtained by comparative methods, *i.e.*, X-ray diffraction, Raman spectroscopy and transmission electron microscopy. Thus, it can be concluded that reflectance indicators such as mean R_{max}, mean R_{min}, bireflectance R_{bi} and Kilby's parameters R_{ev}, R_{st} and R_{am} well illustrate transformation of the structure of coals and other carbonaceous materials. Moreover, they are very sensitive to any changes in dimensions and spatial orientation of the carbon planes that are the basic units of the structure of coals and carbonaceous materials.
- Solely on the basis of reflectance parameters, it could be difficult to determine the absolute degree of structural order of an individual carbonaceous sample. However these parameters appear to be a very good complement to structural studies of coals or carbonaceous materials made by X-ray diffraction or Raman spectroscopy. In cases where a few or more samples are being studied**,** the reflectance parameters examined here will enable even minor differences between the structures of individual samples to be recognized. In addition, optical parameters are able to describe the heterogeneity of the sample in the case of coexisting of components of different optical character, e.g. uniaxial or biaxial, in a single sample.

References

Alpern, B., Lemos de Souza, M.J., 1970. Sur le pouvoir reflecteur de la vitrinite et de la fusinite des houilles Comptes rendus de l'Academie de Sciencesde Paris, 271, 946-959.

Bertrand, R., Malo, M., 2012. Dispersed organic matter reflectance and thermal maturation in four hydrocarbon exploration wells in the Hudson Bay Basin: regional implication. Geological Survey of Canada, Open File 7066, 52p. doi: 10.4095/289709

Beyssac, O., Goffe, B., Petitet. J-P., Froigneux, E., Moreau, M., Rouzaud, J-N., 2003. On the characterization of disordered and heterogeneous carbonaceous materials by Raman spectroscopy. Spectrochimica Acta Part A 59, 2267-2276,

Blanche, C., Dumas, D., Rouzaud, J.N., 1995. The microtexture of anthracites: a key to understand their graphitizability. In: Pajares, J.A., Tascón, J.M.D. Eds.) Coal Science, vol. 1, Elsevier, Amsterdam, pp. 43-46.

Borrego, A. G., Martin, A. J. 2010. Variation in the structure of anthracite at a fast heating rate as determined by its optical properties: An example of oxy-combustion conditions in a drop tube reactor. Int. J. Coal Geol. 81, 301-308.

Chruściel, Z., 1981. New indicator for estimation of metamorphism degree of bituminous coals. (in Polish) Przegląd Górniczy 38, 592-596.

Cook, A.C., Murchison, D.G., Scott, E., 1972. Optical biaxial anthracitic vitrinites. Fuel 51, 180-184.

Davis, A., 1978. The reflectance of coal. In: Karr, C. (Ed.), Analytical Methods for Coal and Coal Products, Vol. 1. Academic Press, New York, pp. 27-78.

Duber, S., Pusz, S., Kwiecińska, B.K., Rouzaud, J.N., 2000, On the optically biaxial character and heterogeneity of anthracites. Int. J. Coal Geol. 44, pp. 227-250,

Goodarzi, F., Murchison, D.G., 1978. Influence of heating rate variation on the anisotropy of carbonized vitrinites. Fuel 57, 273-284.

Goodarzi, F., 1985. Optical properties of vitrinite carbonized at different pressure. Fuel 64, 156-162.

Grieve, D.A., 1991. Biaxial vitrinite reflectance in coals of the Elk Valley coalfield, southeastern British Columbia, Canada. Int. J. Coal Geol. 19, 185-200.

Guedes, A., Valentim, B., Prieto, A.C., Rodrigues, S., Noronha, S., 2010. Micro-Raman spectroscopy of collotelinite, fusinite and macrinite. Int. J. Coal Geol. 83, 415-422,

Hevia, V., Virgos, J.M., 1977. The rank and anisotropy of anthracites: the indicating surface of reflectivity in uniaxial and biaxial substances. J. Microscopy 109, 23-28.

Hower and Davis, 1981a. Vitrinite reflectance anisotropy as a tectonic fabric element. Geology 9, 165-168.

Hower, J., Davis, A., 1981b. Application of vitrinite reflectance anisotropy in the evaluation of coal metamorphism. Geol. Soc. of America Bulletin, Part I, 92, 350-366.

International Committee for Coal and Organic Petrology (ICCP) 2014. Webpage http://www.iccop.org/accreditation/statistical-evaluation-in-detail/ . Accessed in 11.01.2014

Jenkins B.M., 2003. Calibration of image analysis systems for statistically demanding QM application. Microsc Microanal 9, 750-751,

Kalkreuth, W., McMechan, M., 1996. Coal rank and burial history of Cretaceous-Tertiary strata in the Grande Cache and Hinton areas, Alberta, Canada: Implications for fossil fuel exploration. Canadian Journal of Earth Sciences 33, 938-957.

Kilby, W.E., 1988. Recognition of vitrinite with non-uniaxial negative reflectance characteristics. Int. J. Coal Geol. 9, 267-285.

Kilby, W.E., 1991. Vitrinite reflectance measurement - some technique enhancements and relationships. Int. J. Coal Geol. 19, 201-218.

Langenberg, W., Kalkreuth, W., 1991. Reflectance anisotropy and syn-deformational coalification of the Jewel seam in the Cadomin area, Alberta, Canada. Int. J. Coal Geol. 19, 303-317.

Laxminarayana, C., Crosdale, P.J., 1999. Role of coal type and rank on methane sorption characteristics of Bowen Basin, Australia coals . Int. J. Coal Geol. 40, 309-325.

Levine, J.R., Davis, A., 1989. Reflectance anisotropy of Upper Carboniferous coals in the Appalachian foreland basin, PA, USA. Int. J. Coal Geol. 13, 341-373.

Li, M.W., Stasiuk, L., Maxwell, R., Monnier, F., Bazhenova, O., 2006. Geochemical and petrological evidence for Tertiary terrestrial and Cretaceous marine potential petroleum

source rocks in the western Kamchatka coastal margin, Russia . Organic Geochemistry 37, 304-320.

McCartney, J.T., Teichmüller, M., 1972. Classification of coals according to degree of coalification by reflectance of the vitrinite component. Fuel 51, 64-68.

Morga, R., 2011. Micro-Raman spectroscopy of carbonized semifusinite and fusinite. Int. J. Coal Geol. 87, 253-267,

Murchison, D.G., 1978. Optical properties of carbonized vitrinites. In: Karr, C. (Ed.) Analytical methods for coal and coal products, Vol. 2, Academic Press, New York,pp. 415-464.

Oberlin, A., 1984. Carbonization and graphitization. Carbon 22, 521-541.

Potgieter-Vermaak, S., Maledi, N., Wagner, N., Van Heerden, J.H.P., Van Grieken, R., Potgieter, J.H., 2011. Raman spectroscopy for the analysis of coal: a review. J Raman Spectroscopy 42, 123-129.

Pusz, S., Duber, S., Kwiecińska, B.K., 2002, The study of textural and structural transformations of carbonized anthracites, Fuel Proc. Tech. 77-78, 173 -180.

Pusz, S., Kwiecińska, B.K., Duber, S., 2003, Textural transformation of thermally treated anthracites. Int. J. Coal Geol. 54, 115-123.

Rodrigues, S., Suarez-Ruiz, I. Marques, M., Camean, I., Flores, D. 2011. Microstructural evolution of high temperature treated anthracites of different rank. Int. J. Coal Geol. 87, 204-211.

Rodrigues S, Marques M, Suarez-Ruiz I, Camean I, Flores D, Kwiecinska B.. 2013. Microstructural investigations of natural and synthetic graphites and semi-graphites. Int. J. Coal Geol. 111, 67-79.

Ross, J.V., Bustin R.M., 1997. Vitrinite anisotropy resulting from somple shear experiments at high temperature and high confining pressure. Int. J. Coal Geol. 33, 153-168.

Rouzaud, J.-N., Oberlin, A.,1990. The characterization of coals and cokes by transmission electron microscopy. In: Charcosset, H. (Ed.), Advanced Methodologies in Coal Characterization. Elsevier, Amsterdam, pp. 311-355.

Suarez-Ruiz, I., Garcia, A.B., 2007. Optical parameters as a tool to study the microstructural evolution of carbonized anthracites during high temperature treatment. Energy Fuels 21, 2935-2941.

Suarez-Ruiz, I., Crelling, J.C., 2008. Applied Coal Petrology. The Role of Petrology in Coal Utilization. Elsevier, Amsterdam.

Stach, E., Mackowsky, M.Th., Teichmüller, M., Taylor, G.H., Chandra, D., Teichmüller, R., 1982. Stach's Textbook of Coal Petrology. Gebrüder Borntraeger, Berlin.

Stone, I.J., Cook, A.C., 1979, J. Geol. 87, 497-508.

Teichmüller, M., Teichmüller, R., Weber, K., 1979. Inkohlung und Illit-Kristallinität Vergleichende Untersuchungen im Mesozoikum und Paläozoikum von Westfalen. Fortschr. Geol. Rheinlad u. Westf., 27, 201- 276.

Ting, F.T.C., 1981. Uniaxial and biaxial vitrinite reflectance models and their relationship to paleotectonics. In: Brooks, J. (Ed.), Organic Maturation Studies and Fossil Fuel Exploration. Academic Press, London, pp. 379-392.

van Krevelen D.W., 1993. Coal – typology, chemistry, physics, constitution. Third completely revised edition. Elsevier, Amsterdam.

Wilks, K.R., Mastalerz, M., Ross, J.V., Bustin, R.M., 1993. The effect of experimental deformationon the graphitization of Pennsylvania anthracite. Int. J. Coal Geol. 24, 347-369.

ISO 11760:2005(E) – Classification of coals.

ISO 7404-5:1994. Methods for the petrographic analysis of bituminous coal and anthracite.

ASTM D2798 – 11 – Standard Test Method for Microscopical Determination of the Vitrinite Reflectance of Coal.

Caption to the figures

Fig. 1. The relation of principal axes of a RIS to apparent R'_{max} and R'_{min} values.
Fig. 2 Kilby's crossplot for the determination of the RIS principal axes.
Fig. 3 Average maximum (R_{max}) and minimum (R_{min}) reflectances of SV anthracite samples and standard deviation of measurements of apparent R'_{max} and R'_{min} values of the participants for particular temperatures.
Fig. 4 Coefficients of variations (CV) of R_{max} and R_{min} values for particular temperatures.

Fig. 5 The UMSDs of R'_{max} and R'_{min} measurements delivered by the participants.

Fig. 6 Average values and group standard deviations of RIS axes R_{MAX}, R_{INT} and R_{MIN} of SV anthracite samples determined by Kilby's method .
Fig. 7 The course of changes of R_{st} parameter according to increasing temperature of treatment of SV anthracite.

(a) -average values and group standard deviations of R_{st} parameter to the temperature 1650°C.
(b) crossplot of biaxial negative sample (1600 °C).
(c) complex crossplot of the sample containing components of uniaxial (+) and biaxial (-) optical character (1700 °C).

Fig. 8 The UMSDs of the RIS axes.
Fig. 9 The UMSDs of RIS parameters R_{ev}, R_{st}, R_{am} and R_{bi}.
Fig. 10 Similarity of the changes of reflectance parameters (R_{max}, R_{MAX}) and XRD factor L_a under temperature.
Fig. 11 Similarity of the changes of reflectance parameters (R_{min}, R_{MIN}) and XRD factor D_{002} under temperature.
Fig. 12 Similarity of the changes of reflectance anisotropy parameters (R_{bi}, R_{am}) and XRD factors L_a and L_c under temperature.
Fig. 13 The relations between reflectance anisotropy parameters R_{bi} and R_{am} and XRD factor D_{002}.
Fig. 14 Raman spectra of Svierdlovski anthracite heated to different temperatures.
Fig. 15 The relations between reflectance parameters and Raman factors of SV anthracite samples:

(a) R_{min} versus A_{D1}/A_{G1} ratio,
(b) R_{max} versus A_{D1} and A_{G1} values.

Fig.16 TEM micrographs (DF, HRTEM, diffraction pattern) of SV anthracite samples: (a) SV raw, (b) SV 950, (c) SV 1700.

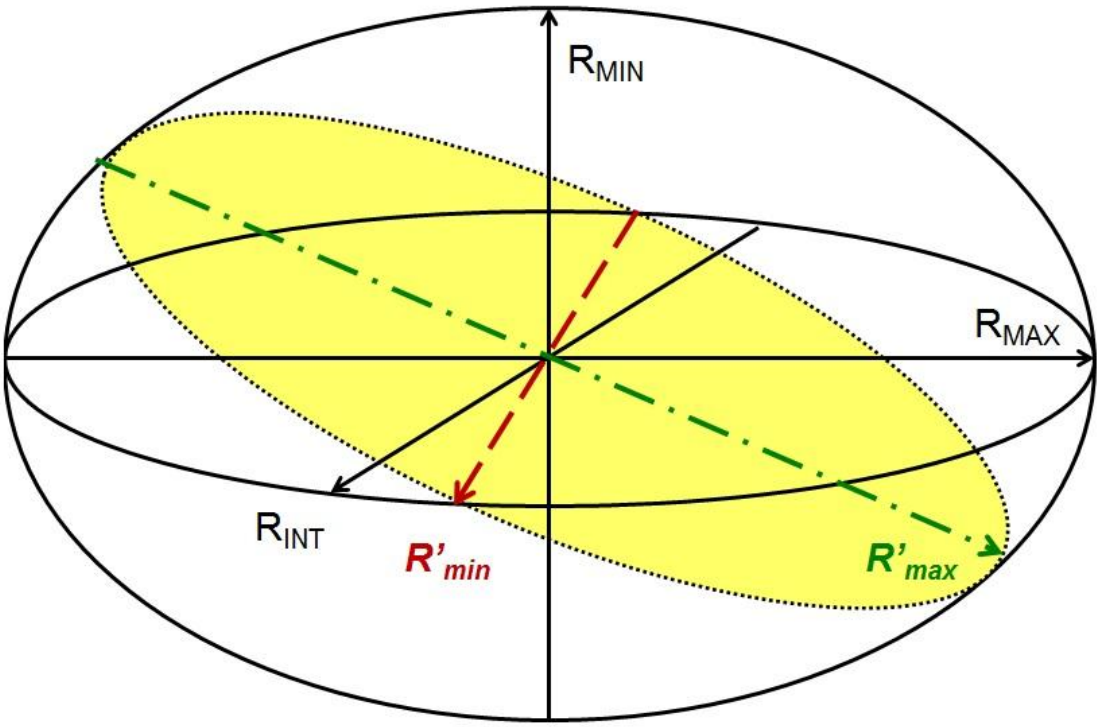

Figure 1

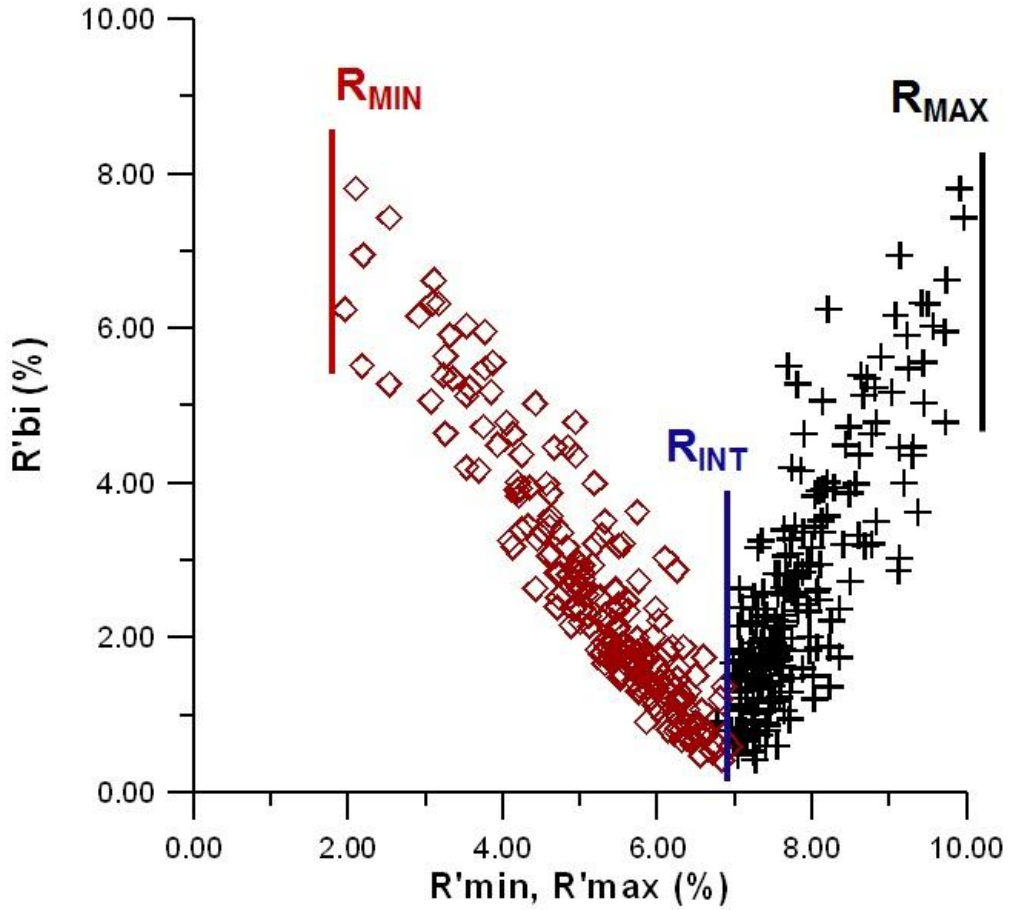

Figure 2

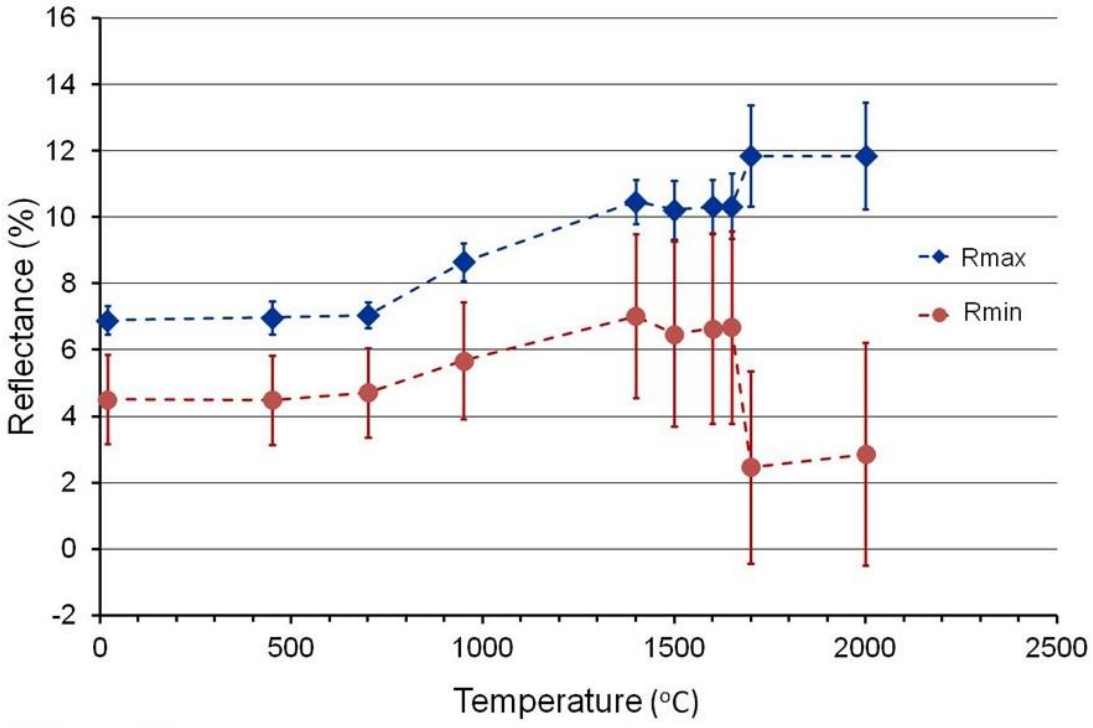

Figure 3

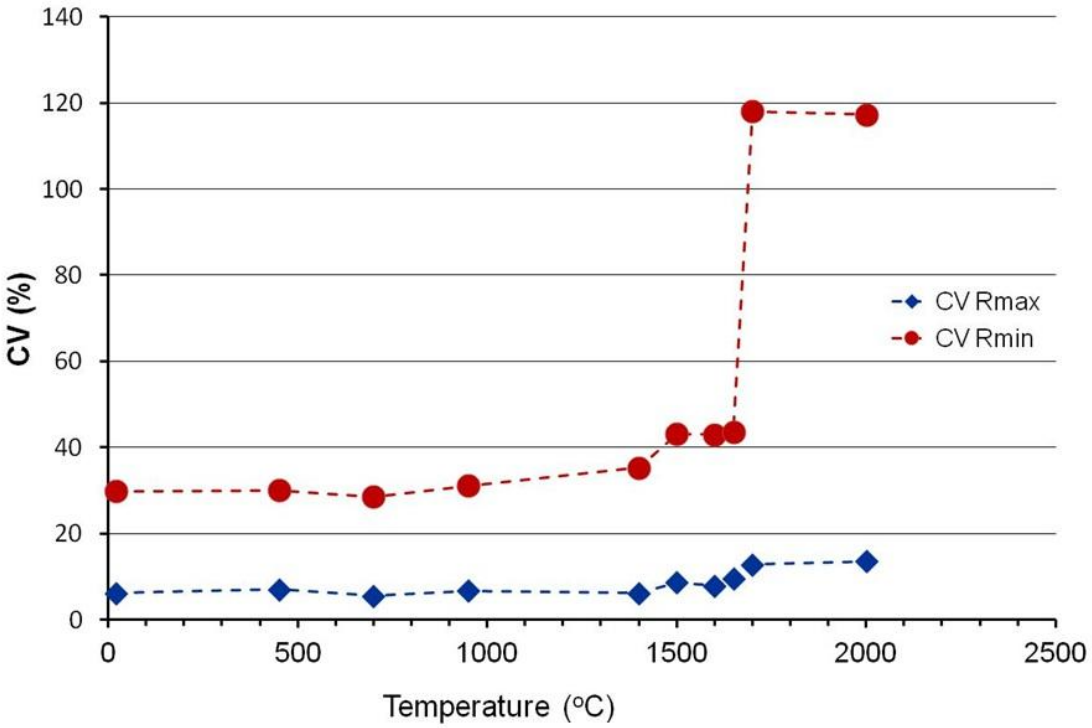

Figure 4

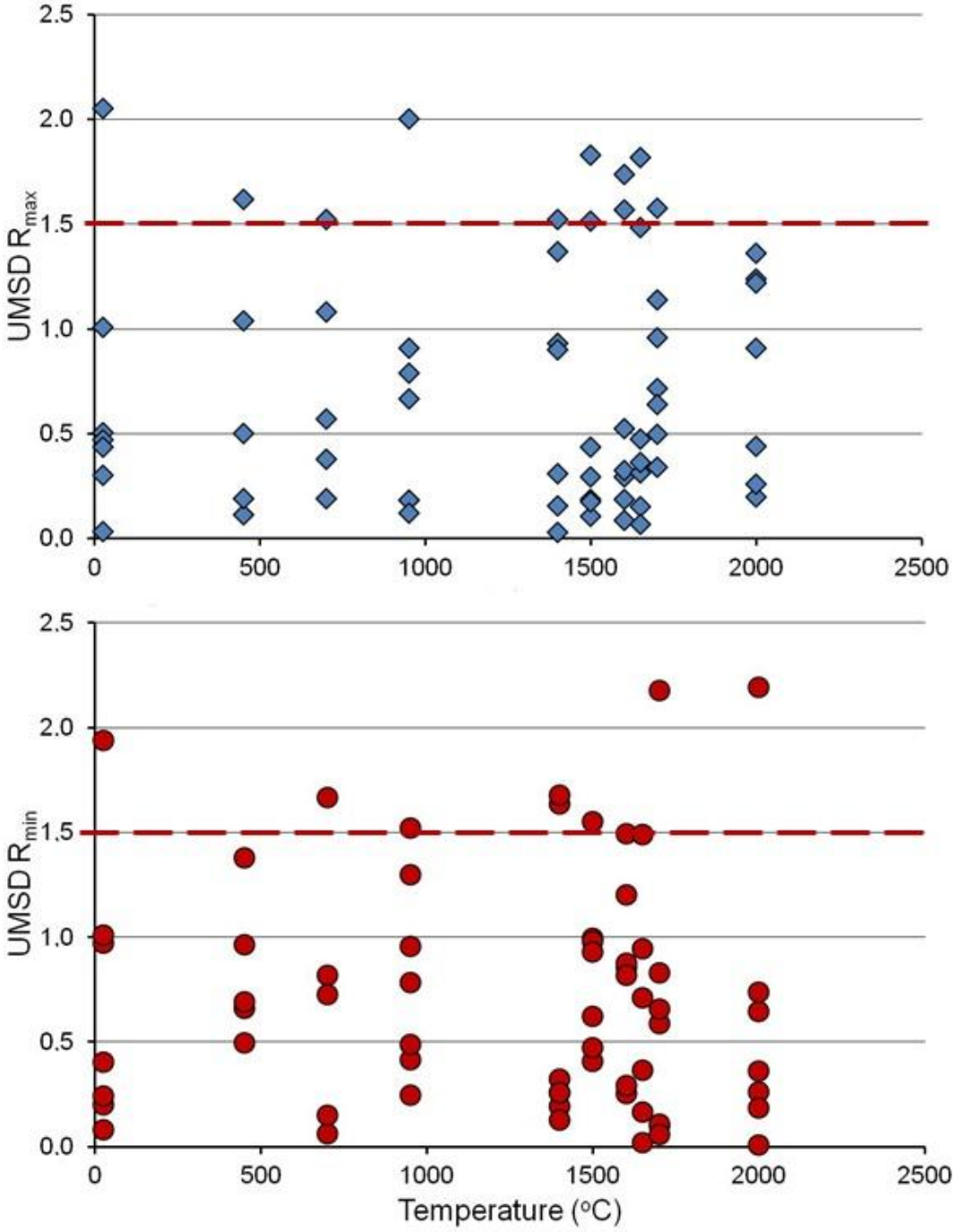

Figure 5

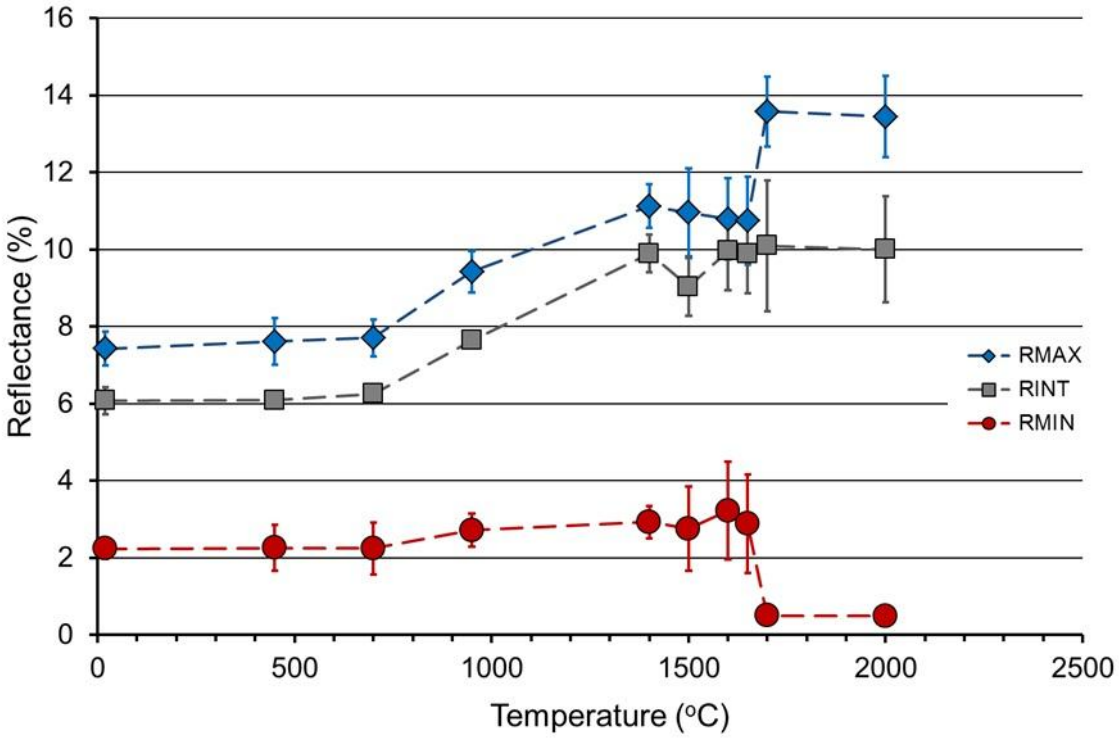

Figure 6

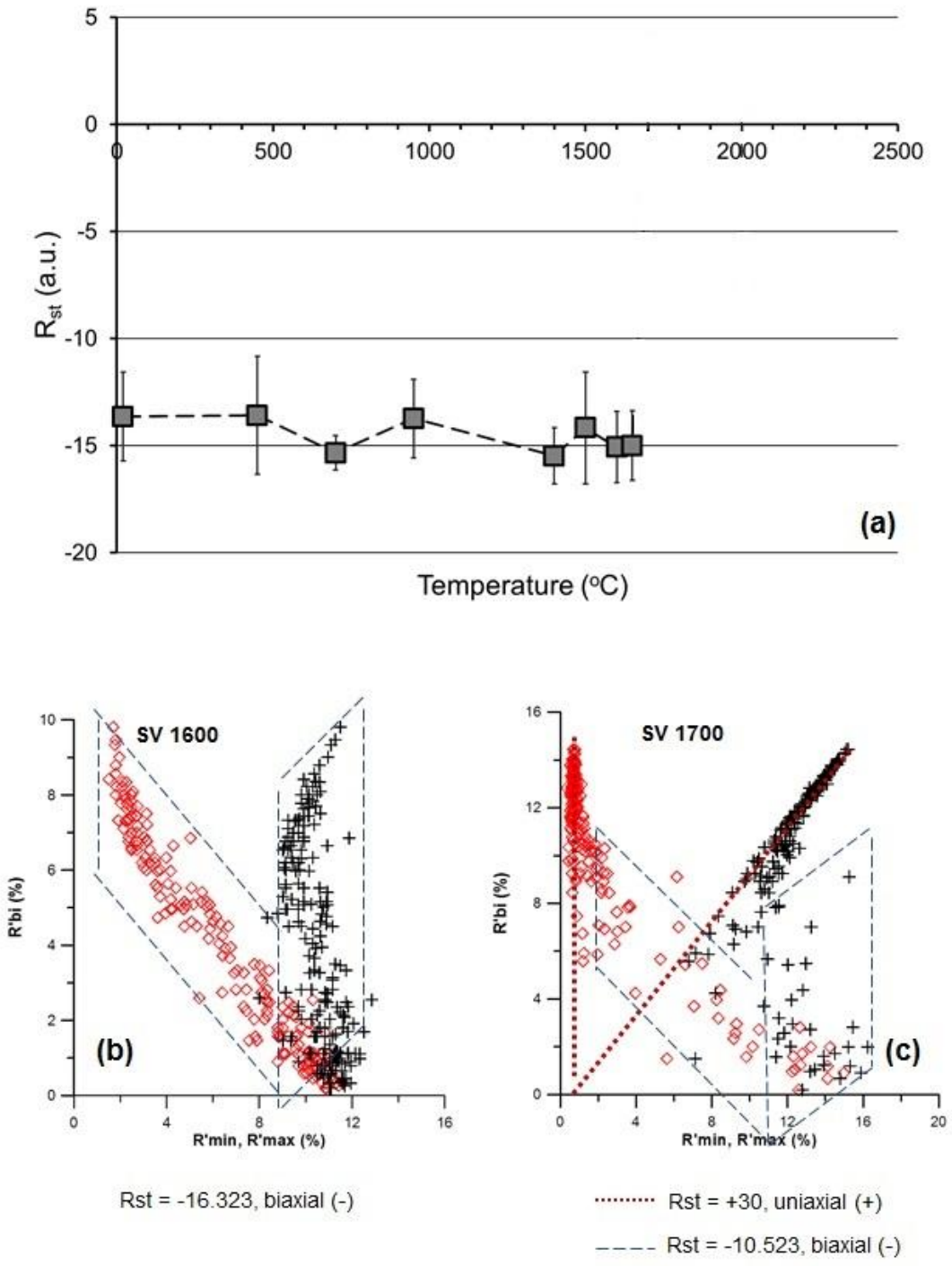

Figure 7

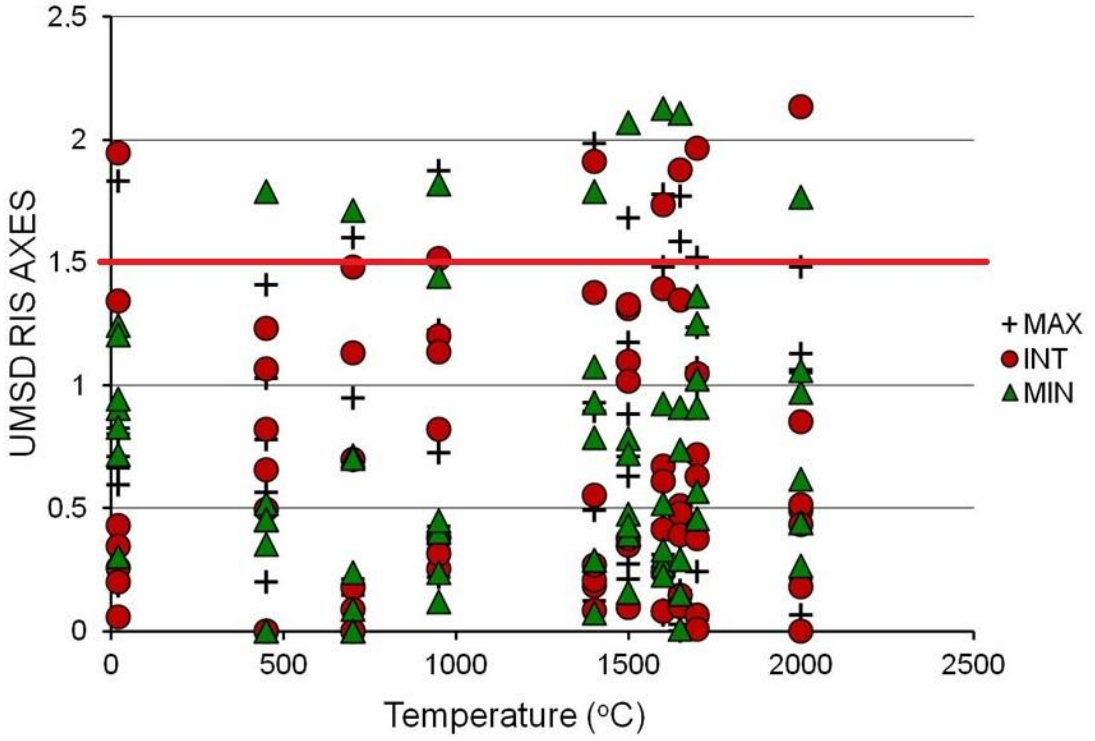

Figure 8

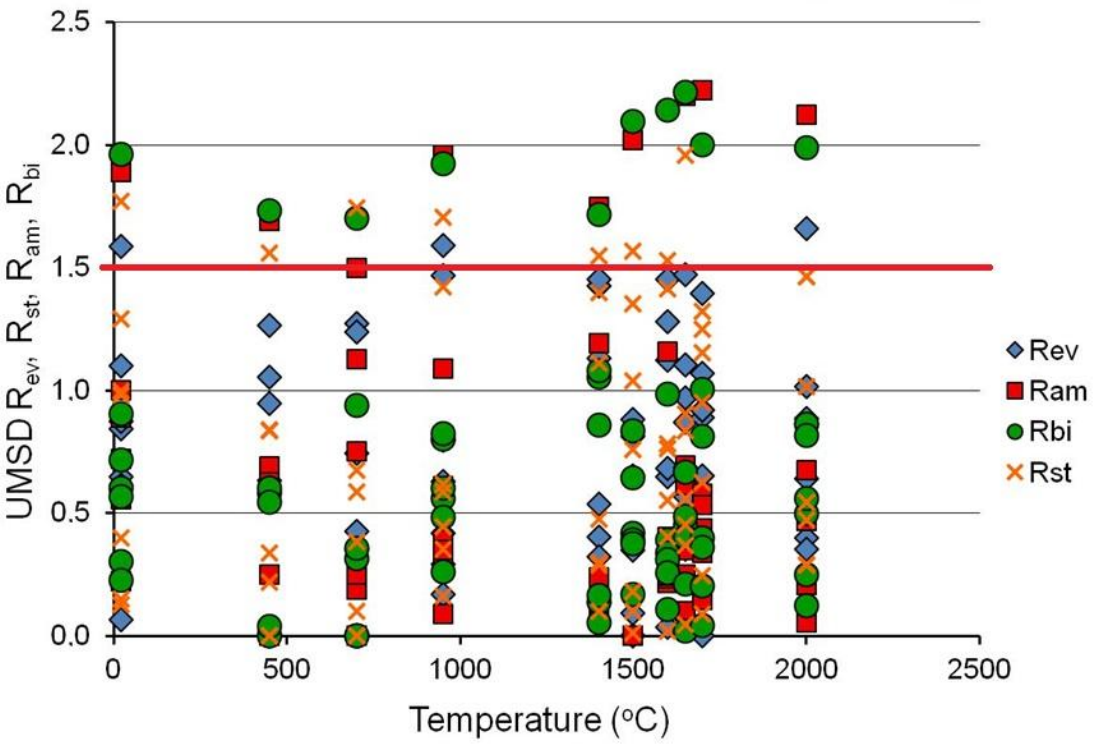

Figure 9

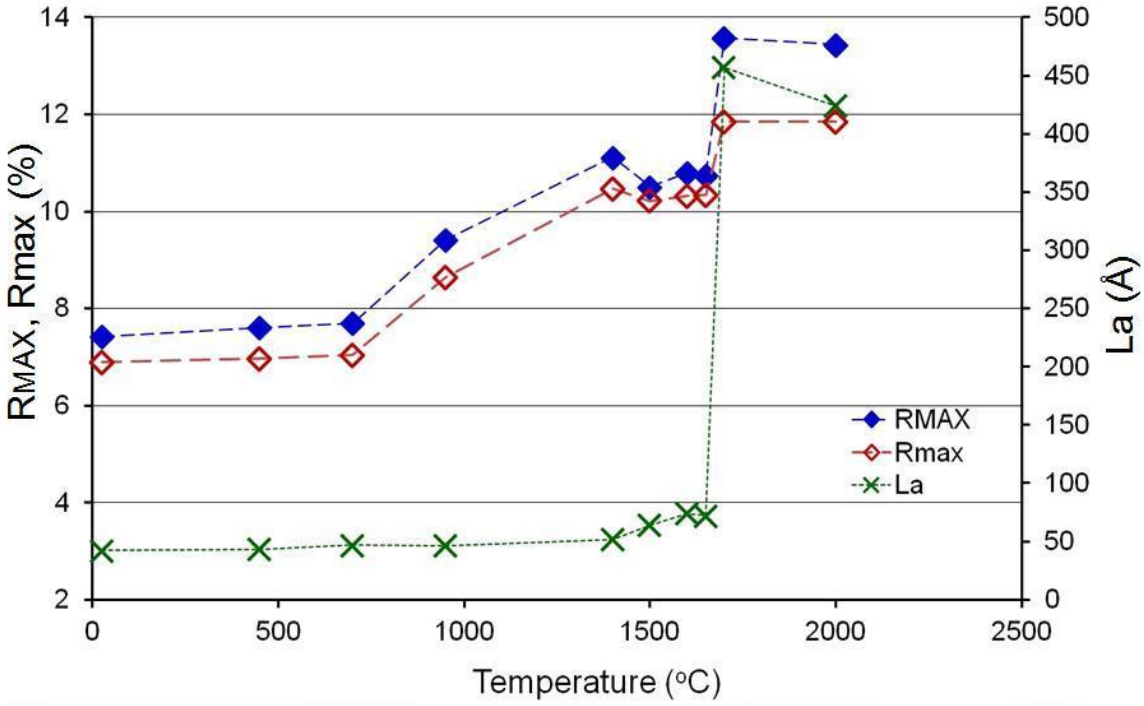

Figure 10

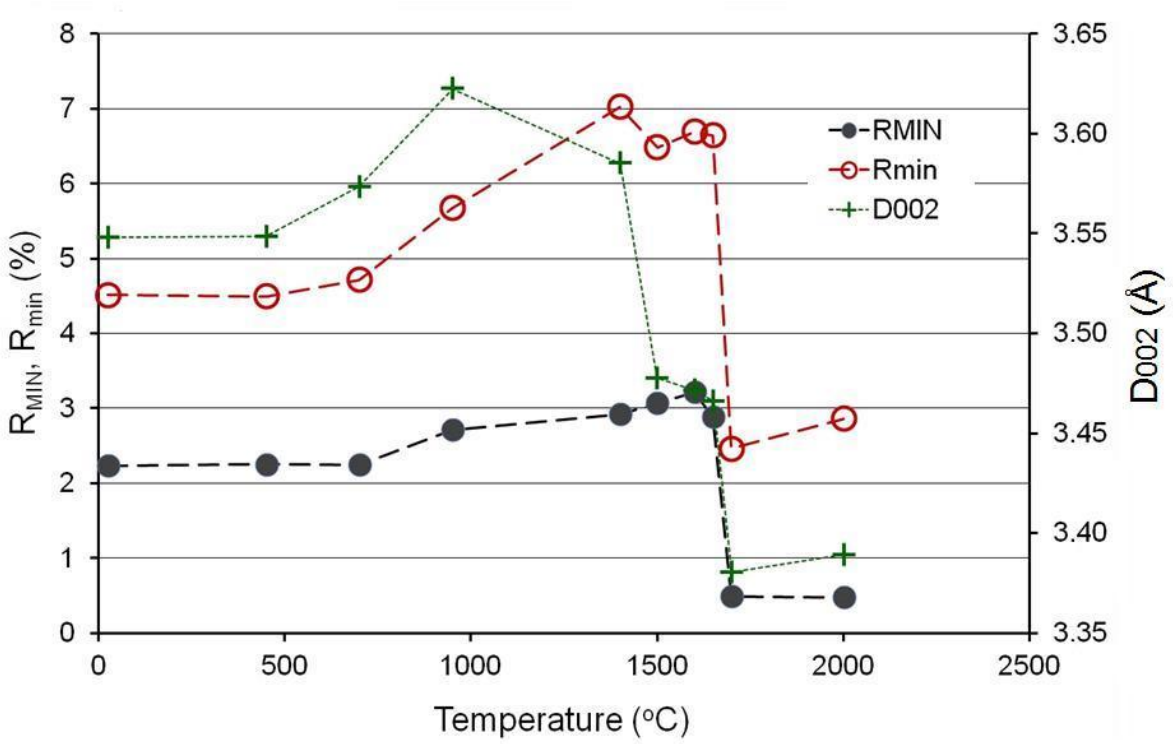

Figure 11

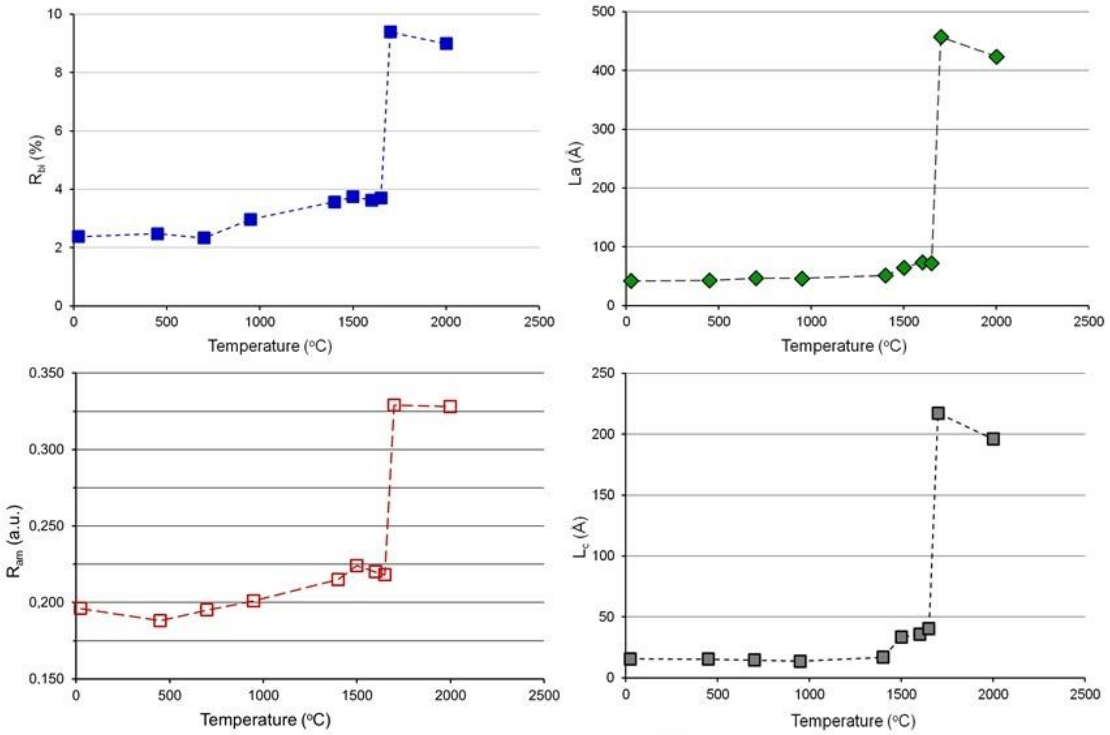

Figure 12

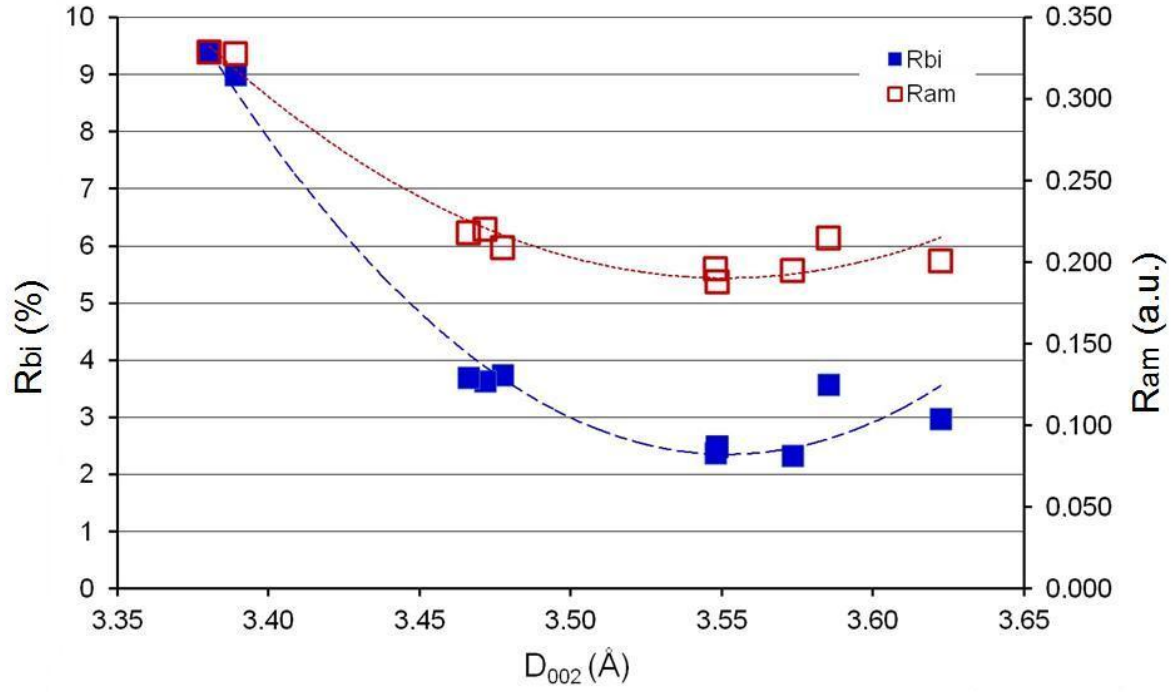

Figure 13

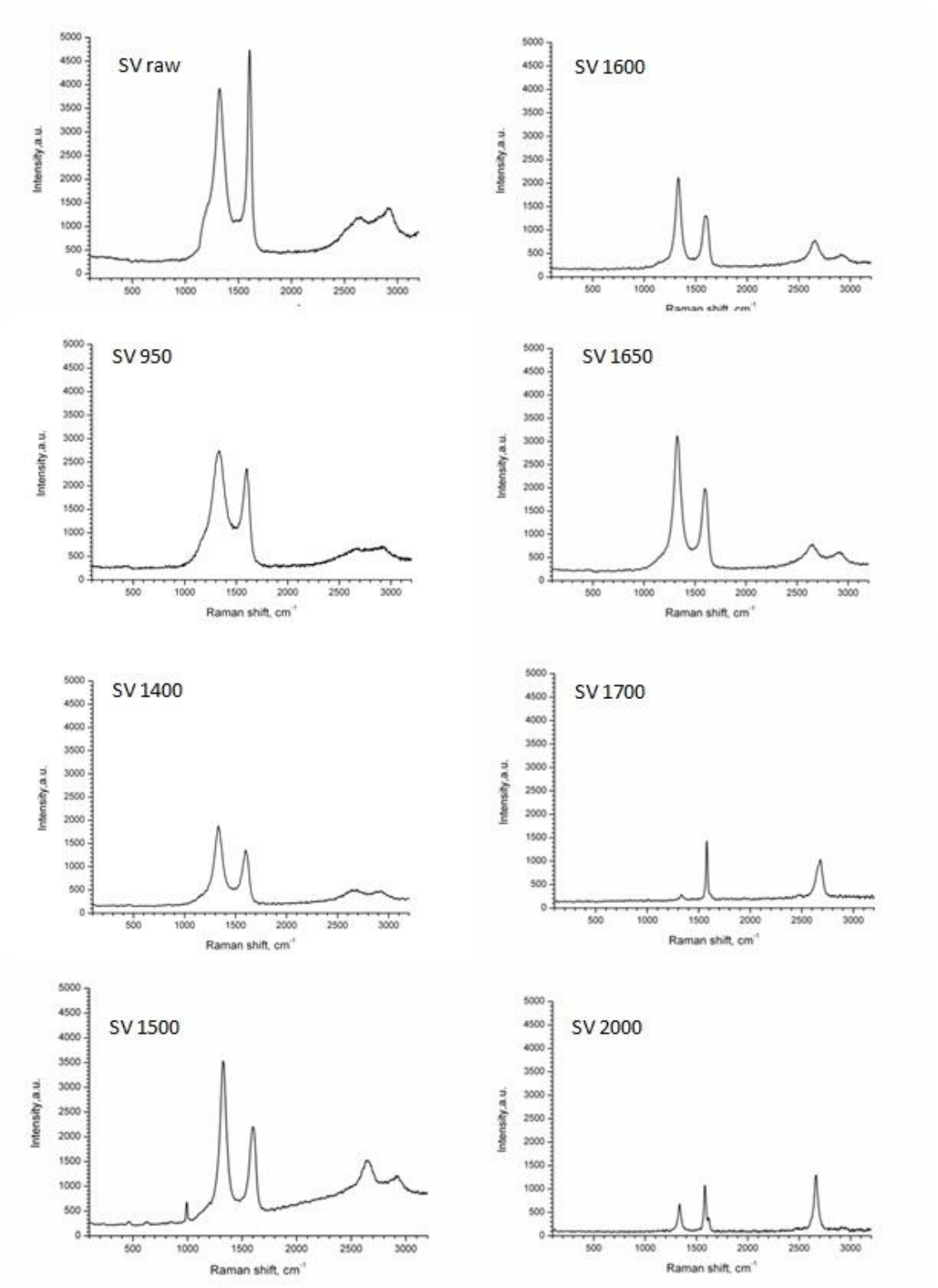

Figure 14

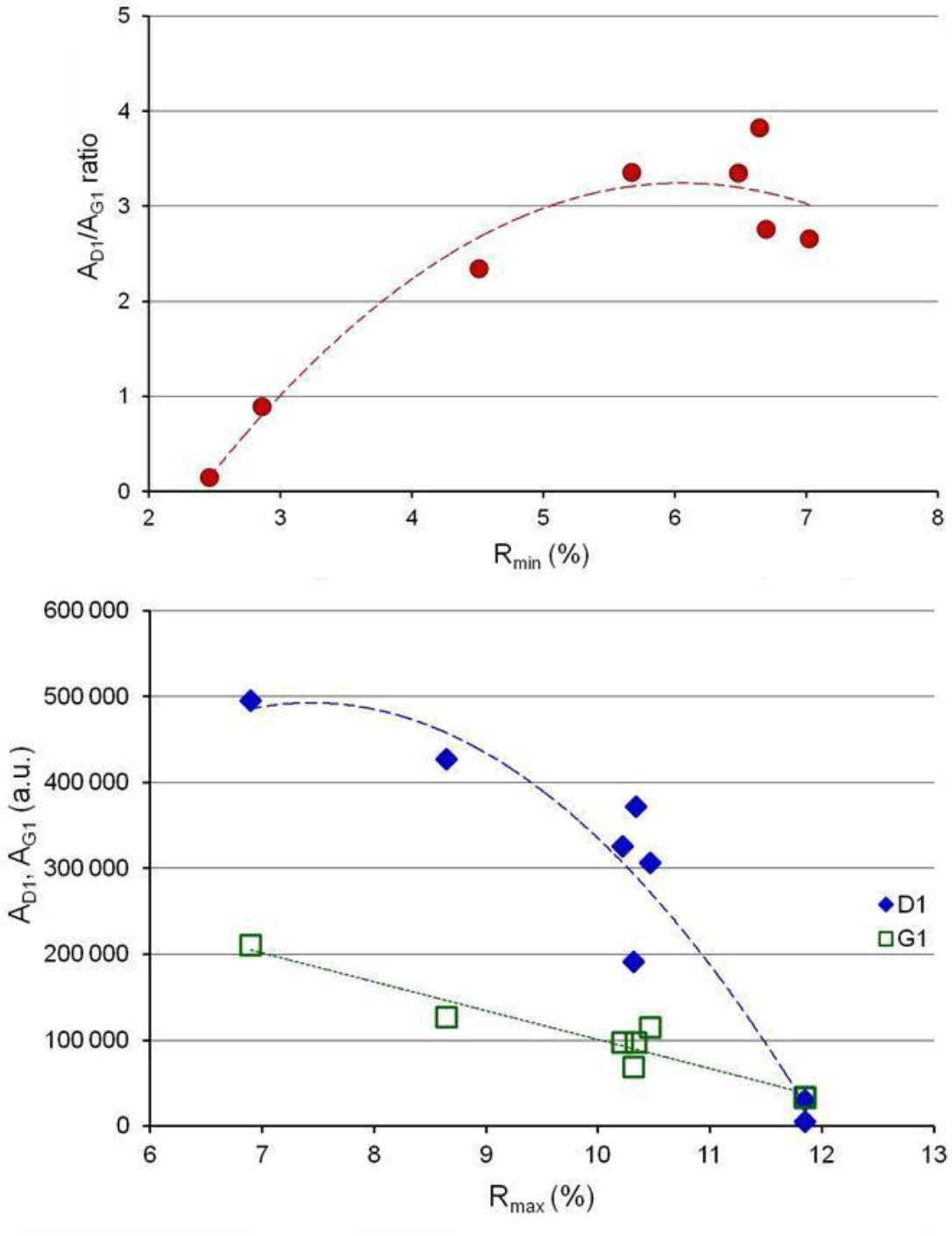

Figure 15

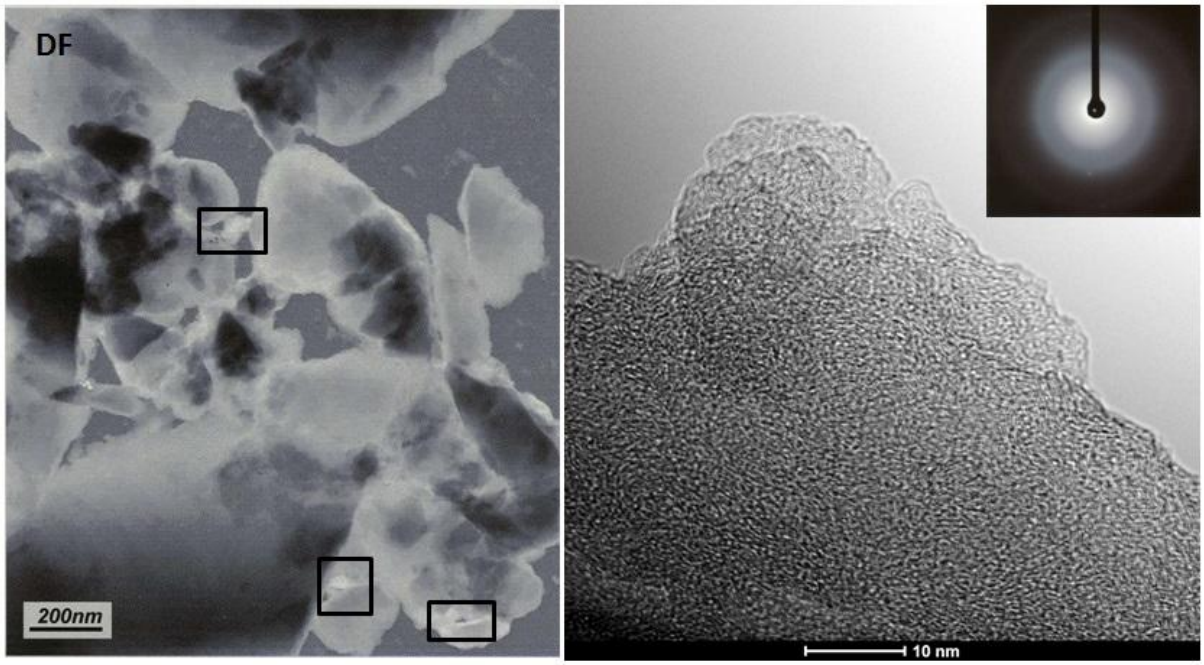

A

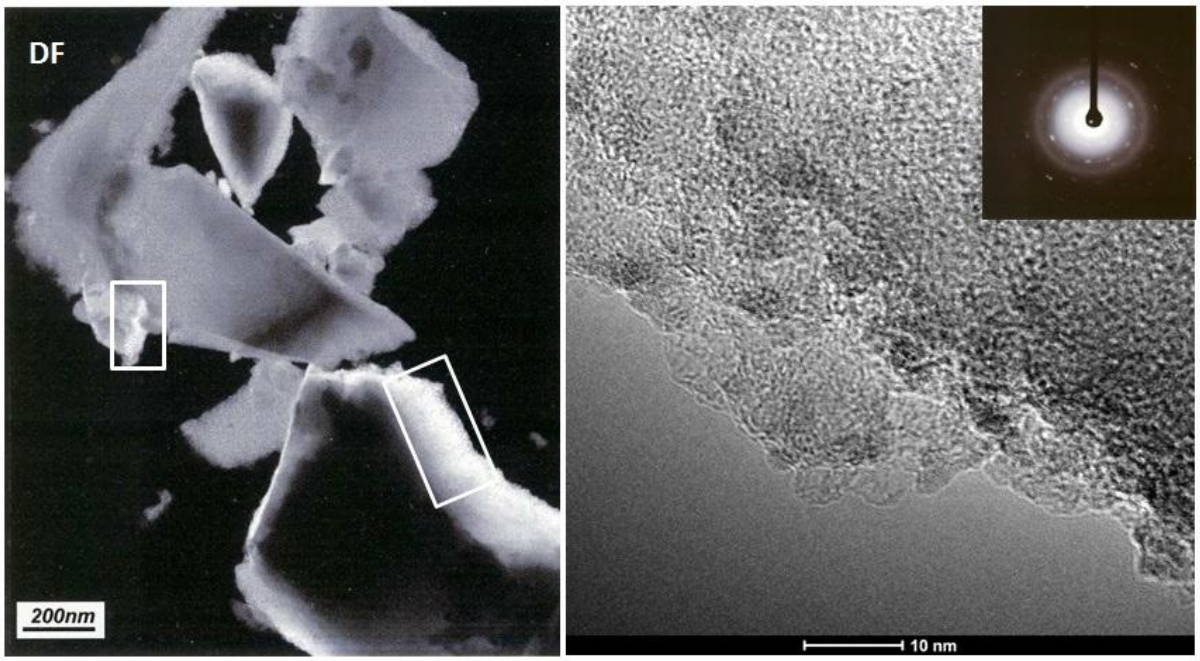

B

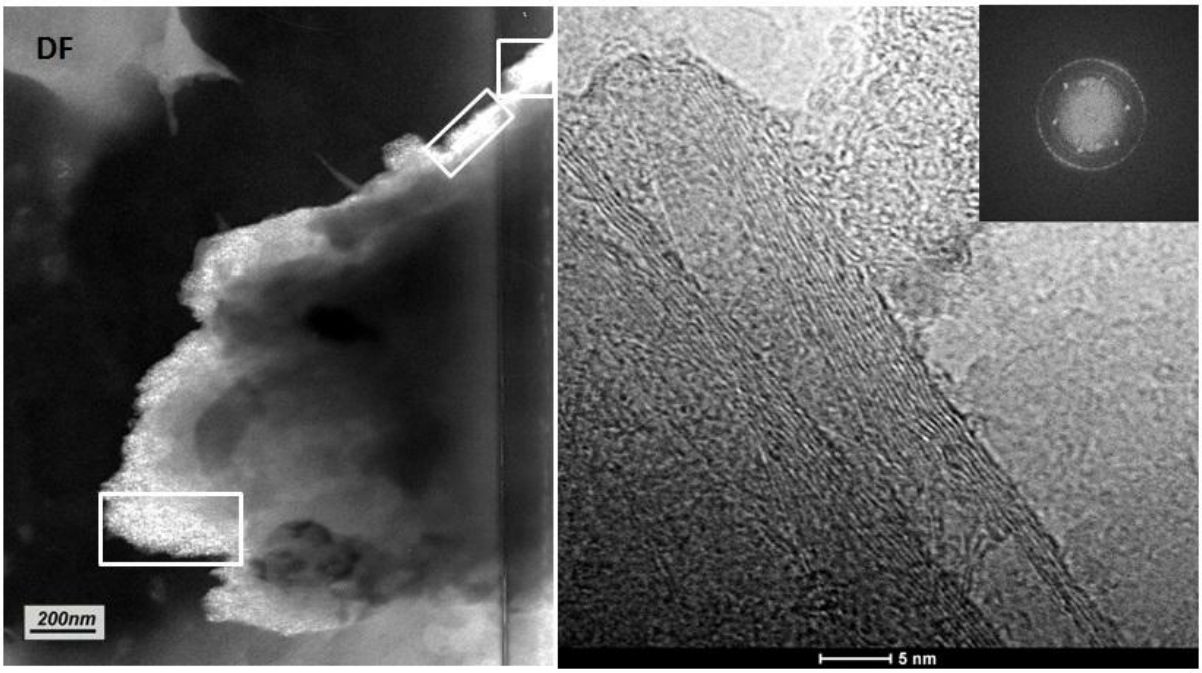

C

Figure 16a-c

Table 1. List of participants (alphabetical order) of the Structural WG and their contribution to round robin exercise.

Participant	Affiliation	Country	Contribution
Sławomira Pusz Convenor	Centre of Polymer and Carbon Materials, Polish Academy of Science, Zabrze	Poland	Arrangement of the exercise Analysis and interpretation of the results R'_{max} and R'_{min}
Diego Alvarez	INCAR-CSIC, Oviedo	Spain	R'_{max} and R'_{min}
Vivien du Cann	Petrog SA, Pretoria	RSA	R'_{max} and R'_{min}
Angeles Gomez-Borrego	INCAR-CSIC, Oviedo	Spain	R'_{max} and R'_{min}
Wolfgang Kalkreuth	University of Rio Grande do Sul, Porto Alegre	Brazil	R'_{max} and R'_{min}
Joanna Komorek	Silesian University of Technology, Gliwice	Poland	R'_{max} and R'_{min}
Jolanta Kus	Geozentrum, Hannover	Germany	R'_{max} and R'_{min}
Barbara Kwiecińska	AGH- University of Science and Technology, Krakow	Poland	R'_{max} and R'_{min}
Manuela Marques	University of Porto, Porto	Portugal	R'_{max} and R'_{min}
Magdalena Misz	University of Silesia, Sosnowiec	Poland	R'_{max} and R'_{min}
Rafał Morga	Silesian University of Technology, Gliwice	Poland	R'_{max} and R'_{min}
Sandra Rodrigues	University of Porto, Porto University of Queensland, St Lucia	Portugal Australia	R'_{max} and R'_{min}
Isabel Suarez-Ruiz	INCAR–CSIC, Oviedo	Spain	R'_{max} and R'_{min}, XRD

Ignacio Camean	INCAR–CSIC, Oviedo	Spain	XRD
Stanisław Duber	University of Silesia, Sosnowiec	Poland	TEM
Marcin Libera	Centre of Polymer and Carbon Materials, Polish Academy of Science, Zabrze	Poland	TEM
Łukasz Smędowski	Institute for Chemical Processing of Coal, Zabrze	Poland	TEM
Joanna Strzezik	Silesian University of Technology, Gliwice	Poland	Raman spectroscopy

Table 2.

Mean maximum (R_{max}) and minimum (R_{min}) reflectance values and standard deviations of apparent R'_{max} and R'_{min} measurements obtained by every participant for Svierdlovski (SV) anthracite samples.

Note: Code numbers used in Tables 2-6 are confidential to the convener.

Sample		Rmax [%]	St.dv.	Rmin [%]	St.dv.
Participant code	**Temperature [°C]**				
2		6.89	0.3975	4.75	1.3966
3	**SV raw**	6.75	0.4378	4.53	1.3211
4		6.76	0.3975	4.46	1.3281
6		6.99	0.3774	4.76	1.4703
10		6.77	0.3807	4.45	1.3079
11		7.51	0.4608	4.61	1.3010
12		6.60	0.5561	4.03	1.3032
Mean		**6.90**	**0.4297**	**4.51**	**1.3469**
2		-	-	-	-
3	SV 450	6.84	0.4421	4.67	1.3224
4		-	**-**	-	**-**
6		7.00	0.3869	4.84	1.5153
10		6.92	0.4079	4.73	1.3716

11		6.70	0.4045	4.24	1.2396
12		7.39	0.7948	3.99	1.3086
Mean		**6.97**	**0.4872**	**4.49**	**1.3515**
2		-	-	-	-
3	SV 700	6.95	0.4047	4.69	1.4205
4		-	**-**	-	**-**
6		7.10	0.3565	4.98	1.5070
10		7.28	0.3576	4.95	1.3273
11		7.01	0.3501	4.76	1.2290
12		6.87	0.4724	4.16	1.2378
Mean		**7.04**	**0.3883**	**4.71**	**1.3443**
2		8.68	0.5151	5.84	1.911
3	SV 950	8.68	0.4979	5.99	1.8610
4		8.50	0.541	5.77	1.8164
6		8.54	0.6113	5.87	1.8399
10		8.63	0.4963	6.06	1.4124
11		8.52	0.5682	5.14	1.7568
12		8.98	0.8084	5.05	1.7508
Mean		**8.65**	**0.5769**	**5.67**	**1.7640**
1		10.37	0.7817	7.11	2.5051
2	SV 1400	10.46	0.6766	6.87	2.6611
3		10.52	0.7454	6.90	2.6091
6		10.77	0.720	7.14	2.595
7		10.18	0.5301	6.23	2.3386
8		10.96	0.6531	7.80	2.3627
9		10.03	0.5533	7.08	2.1998
Mean		**10.47**	**0.6657**	**7.02**	**2.4673**

2		10.47	0.802	6.23	2.9539
3	**SV**	10.31	0.8381	6.1	3.1857
	1500				
5		8.66	1.4156	7.43	1.8276
6		10.38	0.8015	5.87	2.9106
7		11.51	0.7446	6.77	3.1966
8		10.37	0.8541	7.08	2.8936
9		9.85	0.7566	5.91	2.5914
Mean		**10.22**	**0.888**	**6.48**	**2.794**
2		10.62	0.8589	6.55	3.2294
3	SV 1600	10.23	0.884	6.22	2.7474
5		8.56	1.3481	7.35	1.7106
6		10.51	0.8777	6.53	3.2674
7		11.91	0.8683	7.17	3.4820
8		10.65	0.8998	7.14	3.0349
9		9.79	0.7551	5.87	2.6525
Mean		**10.32**	**0.814**	**6.69**	**2.875**
2		10.84	0.9295	6.65	3.2241
3	SV 1650	10.18	0.8172	6.25	2.7626
5		8.44	1.5053	7.16	1.7706
6		10.67	0.8498	6.44	3.3931
7		11.89	0.9734	7.46	3.4984
8		10.41	0.9253	6.73	2.8817
9		9.96	0.8525	5.82	2.7529
Mean		**10.34**	**0.979**	**6.64**	**2.898**
1		11.60	1.2562	1.76	2.3155
2	SV 1700	11.68	1.6023	2.34	3.3612

3		12.21	1.1687	1.68	1.7479
6		12.64	1.735	2.33	3.432
7		11.28	1.3346	1.66	2.3638
8		12.17	1.6728	5.05	4.2167
9		11.37	1.8699	2.39	2.8834
Mean		**11.85**	**1.5199**	**2.46**	**2.9029**
1		12.07	1.4499	2.52	3.4531
2	SV 2000	11.75	1.6598	2.62	3.6371
3		11.98	1.3048	2.02	2.3375
6		12.30	1.556	2.39	3.241
7		11.23	1.7209	2.87	3.4959
8		12.46	1.7869	5.71	5.0618
9		11.17	1.7496	1.90	2.2585
Mean		**11.85**	**1.604**	**2.86**	**3.355**

Table 3. SMSD and AUMSD values of R'max and R'min measurements.

Sample \ Participant	1	2	3	4	5	6	7	8	9	10	11	12	AUMSD
R'max													
SVraw		-0.034	-0.505	0.471		0.303				-0.438	2.054	-1.010	**0.688**
SV450			-0.501			0.116				-0.193	-1.04	1.618	**0.694**
SV700			-0.572			0.381				1.525	-0.191	-1.080	**0.750**
SV950		0.182	0.182	-0.911		-0.668				-0.122	-0.790	2.005	**0.694**
SV1400	-0.311	-0.031	0.155			0.933	0.902	1.524	1.368				**0.746**
SV1500		0.293	0.106		-1.831	0.188	1.514	0.176	-0.434				**0.649**
SV1600		0.296	-0.089		-1.738	0.188	1.571	0.326	-0.524				**0.676**
SV1650		0.477	-0.153		-1.819	0.316	1.484	0.067	-0.364				**0.669**
SV1700	-0.500	-0.34	0.719			1.578	-1.139	-0.639	0.959				**0.839**
SV2000	0.441	-0.200	0.260			0.910	-1.241	1.221	-1.362				**0.805**
AUMSD	**0.421**	**0.232**	**0.324**	**0.691**	**1.796**	**0.558**	**1.309**	**0.659**	**0.835**	**0.570**	**1.019**	**1.428**	**0.820**
R'min													
SVraw		0.970	0.081	-0.202		1.011				-0.243	0.404	-1.941	**0.693**
SV450			0.497			0.966				0.662	-0.690	-1.38	**0.839**
SV700			-0.061			0.818				0.727	0.151	-1.666	**0.685**
SV950		0.417	0.784	0.245		0.49				0.956	-1.299	-1.520	**0.816**
SV1400	0.194	-0.323	-0.258			0.258	-1.635	1.679	0.129				**0.639**
SV1500		-0.408	-0.621		1.551	-0.996	0.474	0.980	-0.931				**0.852**
SV1600		-0.255	-0.856		1.203	-0.292	0.875	0.820	-1.494				**0.828**

SV1650		0.018	-0.709		0.945	-0.364	1.491	0.164	-1.491				**0.740**
SV1700	-0.589	-0.101	-0.656			-0.109	-0.829	2.178	-0.059				**0.646**
SV2000	0.261	-0.185	-0.646			-0.361	0.008	2.192	0.738				**0.627**
AUMSD	**0.348**	**0.335**	**0.517**	**0.224**	**1.233**	**0.567**	**0.885**	**1.336**	**0.807**	**0.647**	**0.636**	**1.627**	**0.763**

Table 4

Reflectance parameters calculated on the base of R'max and R'min measurements.

Sample		RIS axes			Kilby's parameter			
Participant code	Temperature [°C]	R_{MAX}	R_{INT}	R_{MIN}	R_{ev}	R_{st}	R_{am}	R_{bi}
2		7.16	6.09	2.47	4.92	-16.323	0.162	2.14
3	**SV raw**	7.13	5.92	1.98	4.46	-13.898	0.206	2.22
4		7.06	5.95	1.90	4.38	-13.436	0.212	2.30
6		7.77	6.16	2.31	4.91	-13.326	0.183	2.23
10		7.50	6.00	2.55	4.70	-12.813	0.192	2.32
11		8.22	6.75	2.42	5.21	-15.710	0.200	2.90
12		7.11	5.60	2.01	4.45	-9.966	0.214	2.57
Mean		**7.42**	**6.07**	**2.23**	**4.72**	**-13.639**	**0.196**	**2.38**
2		-	-	-	-	-	-	-
3	**SV 450**	7.14	6.00	2.56	4.91	-14.176	0.179	2.17
4		-	-	-	-	-	-	-
6		7.49	6.23	2.52	5.00	-15.887	0.177	2.16
10		7.95	6.02	2.52	4.85	-12.654	0.192	2.19
11		6.99	5.95	2.46	4.79	-15.874	0.178	2.46
12		8.46	6.18	1.18	5.01	-9.298	0.215	3.40
Mean		**7.61**	**6.08**	**2.25**	**4.91**	**-13.578**	**0.188**	**2.48**
2		-	-	-	-	-	-	-
3	**SV 700**	7.25	6.23	2.30	4.79	-15.021	0.192	2.26
4		-	-	-	-	-	-	-
6		7.80	6.38	2.40	4.77	-15.250	0.207	2.12

10		8.46	6.33	2.72	5.25	-16.745	0.191	2.33
11		7.37	6.24	2.71	5.10	-14.857	0.171	2.25
12		7.63	6.08	1.09	4.54	-14.785	0.213	2.71
Mean		**7.70**	**6.25**	**2.24**	**4.89**	**-15.332**	**0.195**	**2.33**
2		9.03	7.83	2.89	6.03	-14.857	0.192	2.84
3	**SV 950**	9.30	7.70	2.54	5.81	-16.323	0.208	2.69
4		8.76	7.40	2.90	5.92	-13.085	0.187	2.73
6		9.60	7.51	2.76	5.98	-12.655	0.193	2.67
10		9.61	7.82	3.32	6.23	-14.018	0.176	2.57
11		9.19	7.60	2.61	5.69	-14.541	0.203	3.38
12		10.43	7.59	1.94	5.50	-10.606	0.246	3.93
Mean		**9.42**	**7.64**	**2.71**	**5.88**	**-13.726**	**0.201**	**2.97**
1		10.96	9.98	3.67	7.22	-15.874	0.193	3.26
2	**SV 1400**	10.59	9.99	2.8	6.65	-14.018	0.214	3.59
3		10.97	10.16	2.89	6.85	-15.348	0.214	3.62
6		11.40	10.56	2.53	6.68	-16.102	0.230	3.63
7		10.61	9.76	2.80	6.60	-17.517	0.213	3.95
8		12.25	9.85	3.25	7.33	-15.859	0.212	3.96
9		11.05	8.96	2.47	6.26	-13.638	0.230	2.95
Mean		**11.12**	**9.89**	**2.92**	**6.80**	**-15.479**	**0.215**	**3.57**
2		12.29	8.77	1.89	5.88	-10.617	0.266	4.24
3	**SV 1500**	10.71	9.85	2.23	5.98	-18.258	0.243	4.21
5		9.03	8.27	5.02	6.87	-16.151	0.135	1.23
6		11.76	8.96	1.96	5.91	-13.898	0.257	4.51
7		11.96	8.05	2.32	6.22	-14.126	0.239	4.74
8		10.64	10.02	3.22	6.87	-11.444	0.206	3.29
9		10.23	9.31	2.58	6.11	-14.628	0.224	3.94

Mean		**10.95**	**9.03**	**2.75**	**6.26**	**-14.160**	**0.224**	**3.74**
2		11.25	10.64	2.83	6.69	-15.021	0.237	4.07
3	**SV 1600**	10.86	9.72	2.88	6.53	-14.392	0.219	4.01
5		8.91	8.2	5.93	7.54	-15.970	0.087	1.21
6		10.88	10.04	2.04	5.98	-16.323	0.247	3.98
7		12.36	11.37	2.8	7.08	-17.402	0.234	4.74
8		11.12	10.38	3.51	7.1	-13.763	0.208	3.51
9		10.16	9.34	2.56	6.07	-12.520	0.31	3.92
Mean		**10.79**	**9.96**	**3.22**	**6.71**	**-15.056**	**0.220**	**3.63**
2		11.25	10.41	1.94	5.96	-13.639	0.255	4.19
3	**SV 1650**	10.72	9.74	2.51	6.16	-15.887	0.233	3.93
5		8.73	7.97	5.56	7.25	-15.060	0.085	1.28
6		10.94	10.38	1.72	5.71	-14.392	0.26	4.23
7		12.56	11.27	2.87	6.95	-18.143	0.239	4.43
8		10.75	9.99	3.07	6.71	-13.526	0.212	3.68
9		10.33	9.49	2.51	5.85	-14.254	0.239	4.14
Mean		**10.75**	**9.89**	**2.88**	**6.37**	**-14.986**	**0.218**	**3.70**
1		13.80	9.98	0.58	4.31	n.d.	0.322	9.84
2	**SV 1700**	12.69	11.31	0.37	3.70	n.d	0.320	9.34
3		13.54	11.16	0.54	4.32	n.d.	0.317	10.53
6		13.60	11.87	0.41	4.01	n.d.	0.321	10.31
7		12.20	10.10	0.45	3.79	n.d.	0.318	9.62
8		14.70	9.45	0.60	4.37	n.d.	0.332	7.12
9		14.55	6.75	0.45	3.54	n.d.	0.375	8.98
Mean		**13.58**	**10.09**	**0.49**	**4.01**	**n.d.**	**0.329**	**9.39**
1		13.37	10.68	0.59	4.38	n.d.	0.315	9.55
2	**SV 2000**	12.32	11.18	0.53	4.16	n.d	0.312	9.13

3	13.66	10.71	0.53	4.27	n.d.	0.319	9.96
6	12.91	10.60	0.41	3.82	n.d.	0.324	9.91
7	12.25	10.00	0.28	3.23	n.d.	0.327	8.36
8	15.00	9.75	0.60	4.44	n.d.	0.332	6.75
9	14.55	7.05	0.45	3.59	n.d.	0.369	9.27
Mean	**13.44**	**10.00**	**0.48**	**3.98**	**n.d.**	**0.328**	**8.99**

Table 5. SMSD and AUMSD values of RIS axes (R_{MAX}, R_{INT}, R_{MIN}) determined from R'_{max} and R'_{min} measurements.

Participant / Sample	1	2	3	4	5	6	7	8	9	10	11	12	AUMSD
R_{MAX}													
Raw		-0.595	-0.663	-0.824		0.801				0.183	1.830	-0.709	**0.801**
SV400			-0.779			-0.199				0.563	1.027	1.408	**0.795**
SV700			-0.947			0.210				1.599	-0.694	-0.147	**0.719**
SV950		-0.724	-0.217	-1.224		0.334				0.353	-0.427	1.874	**0.736**
SV1400	-0.281	-0.930	-0.263			0.491	-0.895	1.983	-0.123				**0.709**
SV1500		1.173	-0.210		-1.681	0.709	0.884	-0.271	-0.630				**0.794**
SV1600		0.434	0.066		1.775	0.085	1.482	0.312	0.595				**0.678**
SV1650		0.438	0.026		1.769	0.166	1.585	0.000	0.368				**0.622**
SV1700	0.242	-0.981	-0.044			0.022	-1.520	1.234	1.069				**0.730**
SV2000	-0.066	-1.062	0.209			-0.503	-1.129	1.480	1.053				**0.786**
AUMSD	**0.196**	**0.792**	**0.342**	**1.024**	**1.742**	**0.352**	**1.249**	**0.880**	**0.640**	**0.675**	**0.995**	**1.035**	
R_{INT}													
Raw		0.057	-0.429	-0.343		0.257				-0.200	1.945	-1.344	**0.654**
SV400			-0.657			1.232				-0.493	-1.067	0.821	**0.854**
SV700			-0.174			1.132				0.697	-0.087	-1.481	**0.714**
SV950		1.199	0.379	-1.515		-0.821				1.136	-0.253	-0.236	**0.791**
SV1400	0.185	0.205	0.554			1.376	-0.267	-0.082	-1.910				**0.654**
SV1500		-0.348	1.099		-1.018	-0.094	-1.313	1.327	0.375				**0.796**
SV1600		0.671	-0.237		-1.736	0.079	1.391	0.414	-0.611				**0.734**

SV1650		0.508	-0.146		-1.875	0.479	1.348	0.098	-0.391				**0.692**
SV1700	-0.065	0.717	0.629			1.046	0.006	-0.376	-1.963				**0.686**
SV2000	0.492	0.853	0.513			0.434	0.000	-0.181	-2.132				**0.658**
AUMSD	**0.247**	**0.570**	**0.482**	**0.929**	**1.543**	**0.695**	**0.721**	**0.413**	**1.230**	**0.632**	**0.838**	**0.971**	
R_{MIN}													
Raw		0.905	-0.942	-1.244		0.302				1.206	0.716	-0.829	**0.878**
SV400			0.518			0.451				0.451	0.351	-1.789	**0.712**
SV700			0.089			0.238				0.715	0.700	-1.713	**0.691**
SV950		0.425	-0.402	0.449		0.118				1.441	-0.236	-1.819	**0.699**
SV1400	1.788	-0.286	-0.072			-0.930	-0.286	0.787	-1.073				**0.746**
SV1500		-0.784	-0.474		2.069	-0.720	-0.392	0.428	-0.155				**0.717**
SV1600		-0.306	-0.267		2.125	-0.925	-0.329	0.227	-0.518				**0.671**
SV1650		-0.738	-0.291		2.105	-0.911	-0.008	0.149	-0.291				**0.642**
SV1700	1.023	-1.364	0.568			-0.909	-0.455	1.250	-0.455				**0.861**
SV2000	0.970	0.441	0.441			-0.617	-1.764	1.058	-0.265				**0.794**
AUMSD	**1.260**	**0.656**	**0.406**	**0.847**	**2.100**	**0.612**	**0.539**	**0.650**	**0.460**	**0.953**	**0.501**	**1.538**	

Table 6. SMSD and AUMSD values of Kilby's parameters R_{ev}, R_{st} and R_{am} and bireflectance R_{bi} calculated from R'_{max} and R'_{min} measurements.

Participant / Sample	1	2	3	4	5	6	7	8	9	10	11	12	AUMSD
R_{ev}													
Raw		0.647	-0.842	-1.101		0.615				-0.065	1.586	-0.874	**0.819**
SV400			0.000			0.947				-0.632	-1.263	1.053	**0.779**
SV700			-0.353			-0.424				1.272	0.742	-1.236	**0.805**
SV950		0.628	-0.293	0.168		0.419				1.466	-0.796	-1.592	**0.766**
SV1400	1.131	-0.404	0.135			-0.323	-0.538	1.427	-1.454				**0.773**
SV1500		-1.080	-0.879		1.357	0.101	-0.276	1.357	-0.553				**0.800**
SV1600		-0.035	-0.315		1.454	-1.278	0.648	0.683	-1.121				**0.791**
SV1650		-0.686	-0.351		1.472	-1.104	0.970	0.569	-0.870				**0.860**
SV1700	0.890	-0.920	0.920			0.000	-0.653	1.069	-1.395				**0.835**
SV2000	0.884	0.398	0.641			-0.354	-1.658	1.017	-0.862				**0.831**
AUMSD	**0.968**	**0.600**	**0.473**	**0.635**	**1.428**	**0.557**	**0.791**	**1.020**	**1.043**	**0.859**	**1.097**	**1.189**	
R_{st}													
Raw		1.292	0.125	-0.980		-0.151				-0.398	0.997	-1.769	**0.816**
SV400			0.218			0.841				-0.337	0.837	-1.559	**0.758**
SV700			-0.384			-0.101				1.744	-0.586	-0.675	**0.698**
SV950		0.618	1.420	-0.351		-0.586				0.160	0.446	-1.706	**0.755**
SV1400	0.300	-1.111	-0.100			0.474	1.549	0.289	-1.339				**0.737**
SV1500		1.354	-1.566		0.760	0.100	0.013	1.038	-0.179				**0.716**
SV1600		0.021	0.401		-0.551	-0.764	-1.415	0.780	1.530				**0.780**

SV1650		0.835	-0.558		-0.046	0.368	-1.957	0.905	0.454			**0.732**
SV1700												
SV2000												
AUMSD	**0.300**	**0.872**	**0.597**	**0.666**	**0.452**	**0.423**	**1.234**	**0.753**	**0.876**	**0.660**	**0.717**	**1.427**	
R_{am}													
Raw		-1.889	0.556	0.889		-0.722				-0.222	0.222	1.000	**0.786**
SV400			-0.563			-0.688				0.250	-0.625	1.688	**0.763**
SV700			-0.188			0.750				0.250	1.500	1.125	**0.763**
SV950		-0.391	0.304	-0.609		-0.348				-1.087	0.087	1.957	**0.683**
SV1400	-1.746	-0.079	-0.079			1.190	-0.159	-0.283	1.190				**0.675**
SV1500		0.957	0.348		-2.000	0.891	0.261	0.457	-0.065				**0.711**
SV1600		0.214	0.327		1.156	0.403	0.232	0.396	0.245				**0.425**
SV1650		0.612	0.248		2.198	0.694	0.347	0.099	0.347				**0.649**
SV1700	-0.338	-0.435	-0.580			-0.386	-0.531	0.145	2.222				**0.662**
SV2000	-0.674	-0.829	-0.466			-0.207	-0.052	0.207	2.124				**0.651**
AUMSD	**0.919**	**0.676**	**0.366**	**0.749**	**1.785**	**0.628**	**0.264**	**0.265**	**1.032**	**0.452**	**0.609**	**1.443**	
R_{bi}													
Raw		-0.905	-0.603	-0.302		-0.566				-0.226	1.961	0.716	**0.754**
SV400			-0.583			-0.602				-0.546	-0.038	1.732	**0.700**
SV700			-0.313			-0.940				0.000	-0.358	1.700	**0.662**
SV950		-0.261	-0.561	-0.481		-0.601				-0.802	0.822	1.925	**0.779**
SV1400	-0.858	0.055	0.138			0.166	1.052	1.079	-1.716				**0.723**
SV1500		0.417	0.392		-2.095	0.643	0.835	-0.376	0.167				**0.704**
SV1600		0.390	0.337		-2.143	0.310	0.983	-0.106	0.257				**0.647**

SV1650		0.449	0.211		-2.216	0.485	0.668	-0.018	0.403				**0.636**
SV1700	0.397	-0.044	1.005			0.811	0.203	-2.001	-0.361				**0.689**
SV2000	0.497	0.124	0.861			0.817	-0.559	-1.988	0.249				**0.728**
AUMSD	**0.584**	**0.331**	**0.500**	**0.392**	**2.151**	**0.594**	**0.717**	**0.928**	**0.526**	**0.394**	**0.795**	**1.518**	

Highlights

1. Accuracy and reproducibility of reflectance measurements were checked.
2. The results turned out to be consistent enough to draw similar conclusions.
3. Reflectance values show good correlations with XRD, TEM and Raman spectroscopy.
4. Reflectance parameters well illustrate structural order of carbonaceous materials.
5. These parameters are a good complement to studies made by XRD or Raman spectroscopy.